RSC Sustainability

ROYAL SOCIETY OF CHEMISTRY

TUTORIAL REVIEW

View Article Online
View Journal | View Issue

Cite this: *RSC Sustainability*, 2024, **2**, 2169

Visible light-induced bromine radical enhanced hydrogen atom transfer (HAT) reactions in organic synthesis

Barakha Saxena, Roshan I. Patel and Anuj Sharma *

Received 2nd May 2024
Accepted 30th June 2024

DOI: 10.1039/d4su00214h

rsc.li/rscsus

Hydrogen atom transfer (HAT) reactions have gained prominence in organic synthesis for providing a straightforward approach towards C–H bond activation for the formation of C-centered radical intermediates. However, halogen radical-assisted hydrogen atom transfer (HAT) reactions have become an interesting tool for C–H bond activation, facilitating the formation of C–C and C–X bonds. In particular, the bromine radical (Br$^{\bullet}$) has garnered attention because of its remarkable capability as a hydrogen acceptor, which abstracts an H-atom from a C–H bond and generates a C-centered radical intermediate. Typically, transition metal- and organo-photocatalysts are commonly used to generate a bromine radical (Br$^{\bullet}$) from a bromine anion (Br^{-}). This newly generated bromine radical (Br$^{\bullet}$) is useful in several organic transformations *via* C–H bond activation. In this review, we provide recent updates on bromine radical (Br$^{\bullet}$) assisted hydrogen atom transfer (HAT) reactions with their scope, mechanism, and limitations.

Sustainability spotlight

In the past few decades, the chemistry of bromine radicals has been well studied, and especially transition-metal-based and heat-assisted radical-based strategies have been well developed. Furthermore, recent advancements in the field of radical chemistry have enabled chemists to explore direct functionalization *via* HAT. Unfortunately, these previous strategies require expensive metals and ligands, high temperatures, and toxic radical initiators, thus making them unsustainable. The development of simple and mild methodologies for bromine radical-enhanced hydrogen atom transfer reactions for the formation of C-centered radical intermediates under visible light is highly desirable. Visible light as an energy source for the reaction reduces the need for harmful UV light and aligns with green sustainable principles for the formation of C–C and C–X bond formation *via* bromine-assisted HAT. Moreover, the developed photocatalytic systems enhance the reaction efficiency and selectivity, making it more sustainable. Photocatalysts like transition metal complexes or organic dyes can activate bromine under visible light irradiation, facilitating the HAT process, which further facilitates C–C and C–X bond formation. Our review emphasizes the importance of the following UN sustainable development goals: affordable and clean energy (SDG 7), industry, innovation, and infrastructure (SDG 9), chemical and waste (SDG 12).

Department of Chemistry, Indian Institute of Technology Roorkee, Roorkee-247667, India. E-mail: anujsfcy@iitr.ac.in; anujsharma.mcl@gmail.com; Tel: +91-1332-284751

Barakha Saxena

Barakha Saxena obtained her BSc (2015) and MSc degrees (2017) in Organic Chemistry from Mahatma Jyotiba Phule Rohilkhand University, Bareilly, Uttar Pradesh, India. She received the Junior Research Fellowship Award (CSIR-JRF) just after completing her Master's. She joined as a PhD scholar in the research group of Prof. Anuj Sharma in the Department of Chemistry, Indian Institute of Technology (IIT), Roorkee, India. She received the Senior Research Fellowship Award (CSIR-SRF). Her current research is focused on novel strategies for C–C and C–X bond formation.

Roshan I. Patel

Roshan I. Patel obtained his BSc (2015) and MSc degrees (2017) in Organic Chemistry from Sardar Patel University, India. He was the gold medalist during his bachelor's degree study. He later joined as a research scholar in Prof. Anuj Sharma's group in the Department of Chemistry, Indian Institute of Technology (IIT), Roorkee, India. His current research is focused on efficient methods for C–H/X functionalization using contemporary methods.

1. Introduction

In synthetic organic chemistry, photocatalysis has undergone significant growth, providing a wide range of useful transformations for accessing valuable organic compounds.[1] Typical photoredox catalysts such as metal photocatalysts (Ru- and Ir-complexes) and organic dyes (eosin Y, rose bengal acridinium-based, *etc.*) have served as popular photocatalysts by harnessing the oxidative/reductive capabilities of both organo-photocatalysts and transition metal (TM) photocatalysts in their activated state. These catalysts efficiently facilitate a broad range of reactions through single electron transfer (SET) or energy transfer (EnT) mechanisms due to their long-excited state lifetimes and useful photoredox potential.[2] Moreover, using substrates or additives capable of forming electron-donor acceptor (EDA) complexes in the ground state have also emerged as an efficient method for C–C and C–X bond formation.[3] In this regard, a new platform has recently emerged that combines photoredox catalysis with halide ion catalysis. They are coordinatively saturated and stable avoiding any ligand exchange with reaction partners.[4] The proposed mechanism is based on a single electron transfer (SET) from the photo-excited catalyst to the halide ion (X^-) to generate a halide radical ($X^\bullet$) that promotes HAT from a substrate C–H bond. A hydrogen atom transfer (HAT) reaction involves the transfer of a hydrogen atom from a hydrogen donor (C–H) to a hydrogen acceptor ($X^\bullet$) and has attracted considerable attention due to its capability for functionalizing complex molecules *via* C–H bond activation.[5] HAT reactions are particularly relevant in the context of radical chemistry, where a radical species ($X^\bullet$) abstracts a hydrogen atom from another molecule, resulting in the formation of a new radical and a different compound. The driving force behind HAT reactions is typically the difference in the stability of the radical intermediates formed before and after the transfer. This process is important in various chemical reactions, including those involved in organic, inorganic, and biological systems (Scheme 1).

Anuj Sharma

Prof. Anuj Sharma earned his PhD from the Institute of Himalayan Bioresource Technology (IHBT) in 2006. Afterward, he undertook two short postdoctoral assignments at UFSM, Santa Maria, in Brazil, in 2006, and KU Leuven, in Belgium, in 2007, before moving to the University of Arizona as a NIH postdoctoral fellow in Prof. Laurence Hurley's group. He is currently working as a professor in the Department of Chemistry, Indian Institute of Technology (IIT), Roorkee, India. His group focuses on developing green organic synthetic methodologies, including visible light driven C–H functionalization.

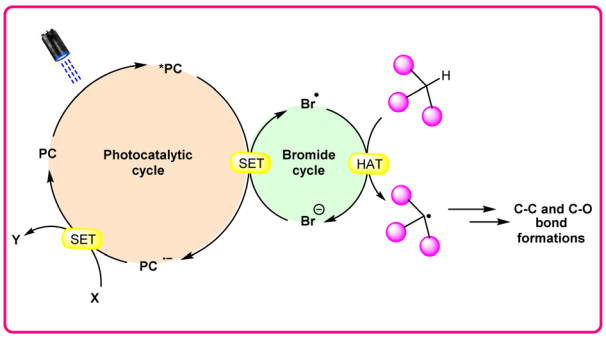

Scheme 1 General approach toward the generation of a bromine radical and the hydrogen atom transfer process.

Consequently, the utilization of a radical reagent capable of forming bonds that are more stable than those to be cleaved can enable direct functionalization *via* HAT. Various radical species ($X^\bullet$), such as O-, N-, S-, B-, and halogen-centered radicals, have been identified as suitable HAT reagents.[6] Among them, halogen radicals have garnered significant interest due to their ease of accessibility and high reactivity.

Halogen radicals, especially the chlorine radical ($Cl^\bullet$) and bromine radical ($Br^\bullet$), serve as potent hydrogen acceptors and play a crucial role as agents for facilitating hydrogen atom transfer (HAT).[7] The bromine radical ($Br^\bullet$) is a highly reactive species with an unpaired electron, which makes it capable of abstracting a hydrogen atom from a nearby molecule, leaving behind hydrogen bromide (HBr). The X–H (X= C, Si) bond dissociation energies (BDEs) of the hydrocarbons listed in Scheme 2 are generally in the vicinity of the bond formation energy of H–Br (87 kcal mol^{-1}).[8] Therefore, the bromine radical ($Br^\bullet$) demonstrates a facile ability to cleave the X–H (X= C, Si) bonds. Conversely, iodine radicals ($I^\bullet$) exhibit minimal to no capability for engaging in C–H bond activation.[8b] There have been significant efforts devoted to C–H bond activation *via* hydrogen atom transfer (HAT), which can be seen in a few excellent review articles.[9] Some of the notable ones are by Ravelli and co-workers in 2020, who discussed direct, indirect, and remote photocatalytic HAT reactions for the formation of C-centered radical intermediate.[9a] However, photocatalytic hydrogen atom transfer (HAT), where halogen radicals are involved in the activation of the C–H bonds, was not discussed by them. Next, in 2022, Capaldo and co-workers published an article on photocatalytic halogen-radical assisted HAT reactions; however, HAT reactions *via* the bromine radical were merely covered.[10] Later, in 2023, Itabashi, Asahara, and Ohkubo presented an excellent review on chloride radical ($Cl^\bullet$)-mediated C–H oxygenation strategies *via* HAT for the formation of the C–O bond.[11]

As per our knowledge, there has been no review article exclusively focused on visible light-mediated hydrogen atom transfer (HAT) reactions using the bromine radical ($Br^\bullet$). Within this framework, the present article is written, addressing strategies involving bromine radical ($Br^\bullet$) mediated hydrogen atom transfer (HAT) under visible light irradiation for the generation

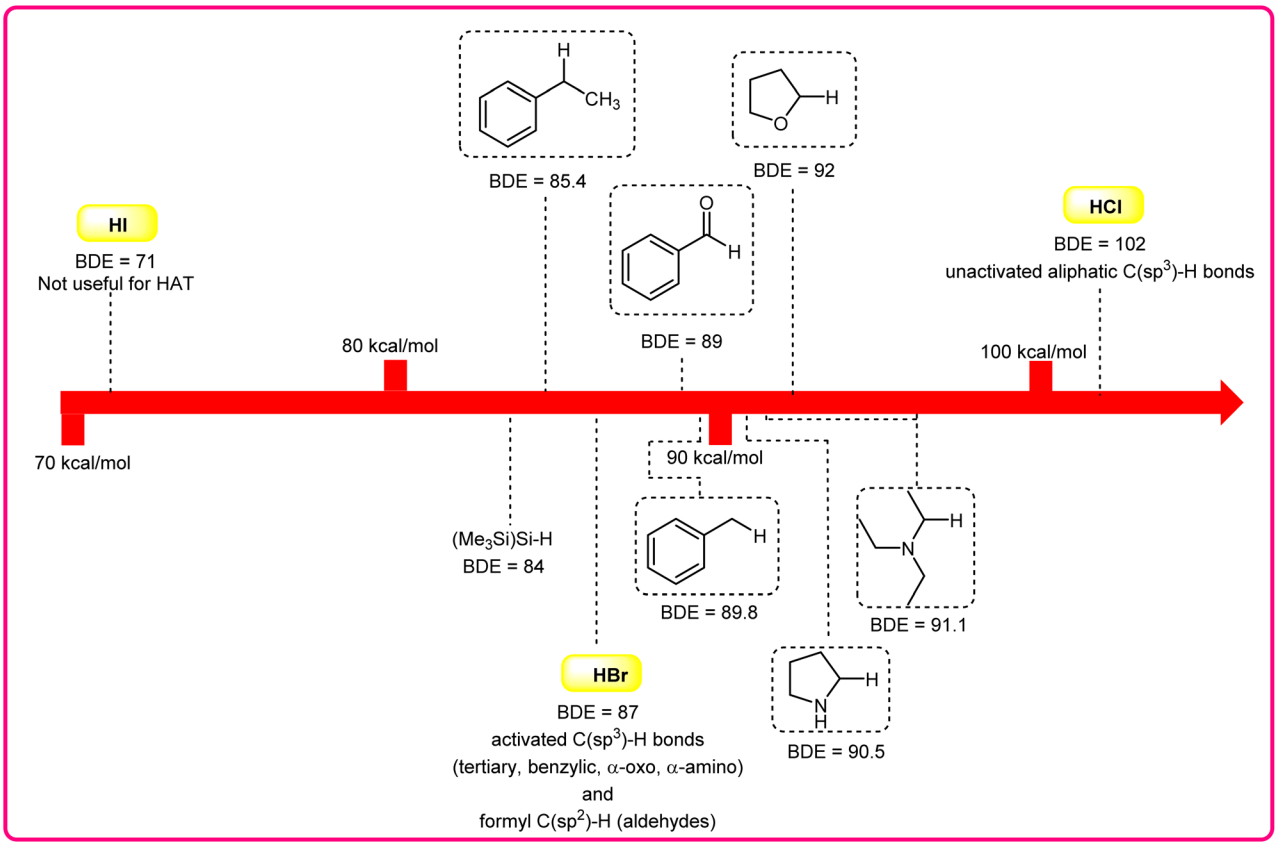

Scheme 2 Bond dissociation energies (kcal mol^{-1}) of C–H bonds and those of H–X bonds.

of C–C and C–O bonds. The contents of the review are categorized into various types of hydrogen atom transfer reactions from the bromine radical (Br$^{\bullet}$), such as (1) hydrogen atom transfer from aldehydes, (2) hydrogen atom transfer from benzylic carbons, (3) hydrogen atom transfer from α-hetero carbons, (4) hydrogen atom transfer from $(Me_3Si)_3SiH$, (5) hydrogen atom transfer from allylic carbons and (6) miscellaneous.

2. Hydrogen atom transfer from aldehydes

Hydrogen atom transfer (HAT) from aldehydes involves the transfer of a hydrogen atom from an aldehyde molecule to another molecule or radical intermediate. The hydrogen atom attached to the carbonyl carbon in aldehydes is relatively acidic due to the electron-withdrawing nature of the carbonyl group. Initially, the HAT reaction is initiated by the generation of a bromine radical (Br$^{\bullet}$), often through the excited photocatalyst (*PC) *via* reductive quenching. This resulting bromine radical (Br$^{\bullet}$) abstracts a hydrogen atom bound to the carbon atom adjacent to the carbonyl group. The abstraction occurs due to the high reactivity of the bromine radical species (Br$^{\bullet}$), which seeks to stabilize itself by pairing its unpaired electron with an electron from the hydrogen atom, thus forming a new covalent bond. Moreover, the abstraction of the hydrogen atom leads to the formation of an acyl radical intermediate, which contains an unpaired electron, making it highly reactive and prone to further chemical reactions. The generation of an acyl radical *via* bromine radical-mediated HAT is shown in Scheme 3.

In 2020, Huang and co-workers reported photoredox Minisci-type alkylation of pyridines **1** with aliphatic and aromatic aldehydes **2** as an umpolung alkylating reagent (Scheme 4).[12] Under optimized conditions, the authors were able to demonstrate the Minisci-type alkylation of some bioactive molecules such as quinoxyfen and fasudil in 40% and 50% yields, respectively. Various mechanistic studies such as H/D exchange, kinetic isotopic effect (KIE) experiments, and Stern–Volmer quenching studies were performed to understand the reaction mechanism. Mechanistically, the photoexcited catalyst *Ir(III) undergoes a single electron transfer (SET) process with

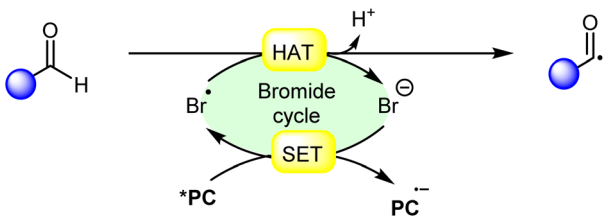

Scheme 3 General approach for acyl radical intermediate formation *via* bromine radical mediated HAT.

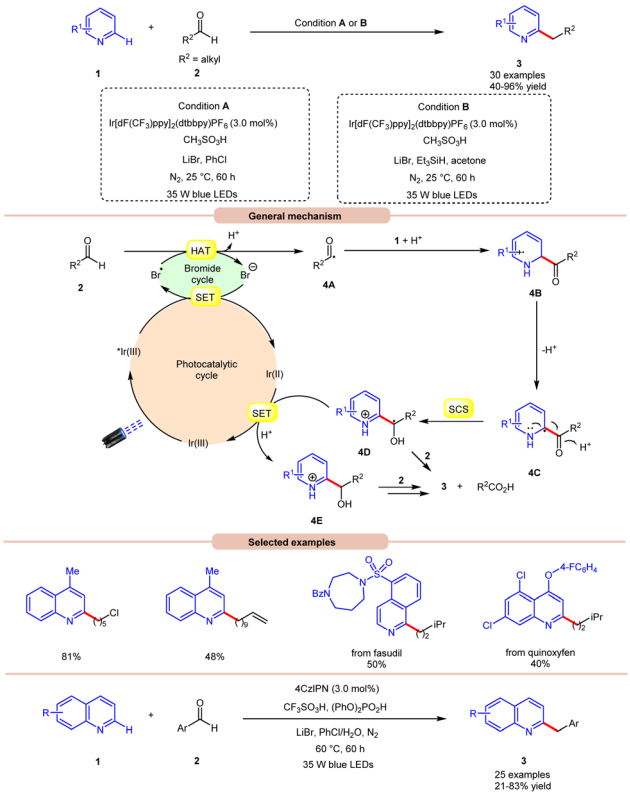

Scheme 4 Ir-catalyzed photoredox Minisci-type alkylation of pyridines.

a bromide ion (Br^-) to generate a bromine radical ($Br^•$) and Ir(II). This bromine radical ($Br^•$) would abstract a hydrogen atom from aldehyde **2** *via* deprotonated electron transfer (DPET) to access the acyl radical **4A**. The resulting intermediate **4A** adds to the *N*-heterocycle **1**, accompanied by deprotonation, and subsequently spin-center shift (SCS) occurs to generate the hydroxyalkyl radical intermediate **4D**. Next, the SET process from the reductive Ir(II) to the intermediate **4D** furnishes the intermediate **4E**. Furthermore, the reduction of **4E** with aldehyde **2** affords the final product **3**. With a change in reaction conditions, the authors further demonstrated the benzylation of nitrogen-containing heteroarenes **1** using benzaldehydes **2** by employing 4CzIPN as the photocatalyst, with CF_3SO_3H and $(PhO)_2PO_2H$ as acids, and LiBr as the additive in chlorobenzene (PhCl) under visible light irradiation, affording the desired products **3** in 21–83% yield.

Wang, Huang, and co-workers in 2020 illustrated dual photoredox/bromide catalyzed Minisci hydroxyalkylation of quinolines **4** using aldehydes **2** under visible light irradiation (Scheme 5).[13] Inexpensive LiBr was chosen as an efficient moderator for this protocol with 4CzIPN as an organophotocatalyst under visible light irradiation.

A range of substituted aldehydes **2** reacted well under the optimized conditions, affording the desired products in moderate to excellent yields. Notably, aliphatic aldehydes **2** remained inactive under the reaction protocol. Deuterium studies indicated the formation of acyl radical *via* C–H scission

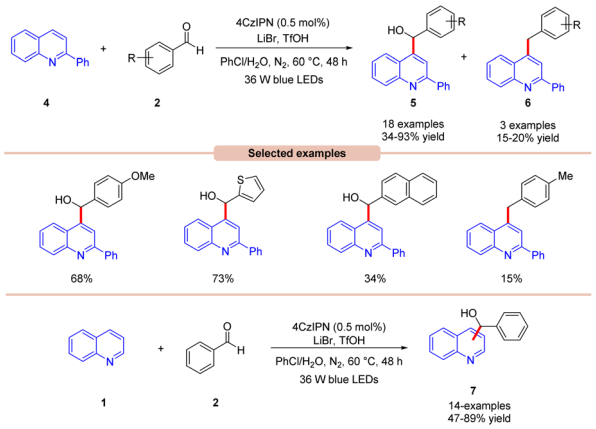

Scheme 5 Dual 4CzIPN/LiBr mediated Minisci hydroxyl alkylation of quinolines with aryl aldehydes.

of aldehyde **2**, which was further proven by the TEMPO trapping experiment. The Stern–Volmer experiment reveals that 4CzIPN could efficiently oxidize the bromide anion, thus forming a bromine radical intermediate. Finally, the light-on-off experiment found that the visible light irradiation is crucial for the reaction protocol. Based on these findings, the authors proposed that the generated bromine radical intermediate undergoes HAT with the aldehyde **2** to form an acyl radical intermediate, which reacts with the quinoline **4**, followed by a similar mechanistic pathway to that described in Scheme 4 to give the final product **5**. Under the same reaction conditions, a broad range of quinolines **1** were also successfully converted to yield the desired hydroxyalkylated product **7**. This protocol is limited to quinolines as it fails to undergo a Minisci-type reaction with benzothiazole, benzo-oxazole, and quinoxalinone.

Oxindoles are quintessential moieties in pharmaceuticals, organic materials, and natural products.[14] Great attention has been given to their synthesis. Deng and co-workers in 2022 established visible light-induced radical alkylation of *N*-arylacrylamides **8** with aliphatic aldehydes **2** (Scheme 6).[15] The authors employed 4CzIPN as a photocatalyst with NaBr as an additive and TBHP as an oxidant under visible light irradiation. Both electron-donating and electron-withdrawing groups at various positions of the aryl ring of *N*-arylacrylamides **8** were well tolerated. Moreover, the aliphatic aldehydes **2** containing cyclic and acyclic groups showed good reactivities under the reaction conditions. A key feature of this strategy was illustrated in the late-stage functionalization of naproxen, ibuprofen ciprofibrate, and probenecid drug molecules. Radical trapping experiments with TEMPO, BHT, or 1,1′-diphenylethylene completely suppressed the reaction, which supported the involvement of a radical mechanistic pathway. Based on these findings and several other controlled experiments, the authors proposed a plausible mechanism, as illustrated in Scheme 6. The photoexcited catalyst 4CzIPN* oxidizes the bromide anion to generate a bromine radical *via* a SET process, which participates in HAT with the aldehyde **2** to form acyl radical intermediate **6A**, followed by carbon monoxide (CO) removal to form an alkyl radical intermediate. Next, the alkyl radical adds to the

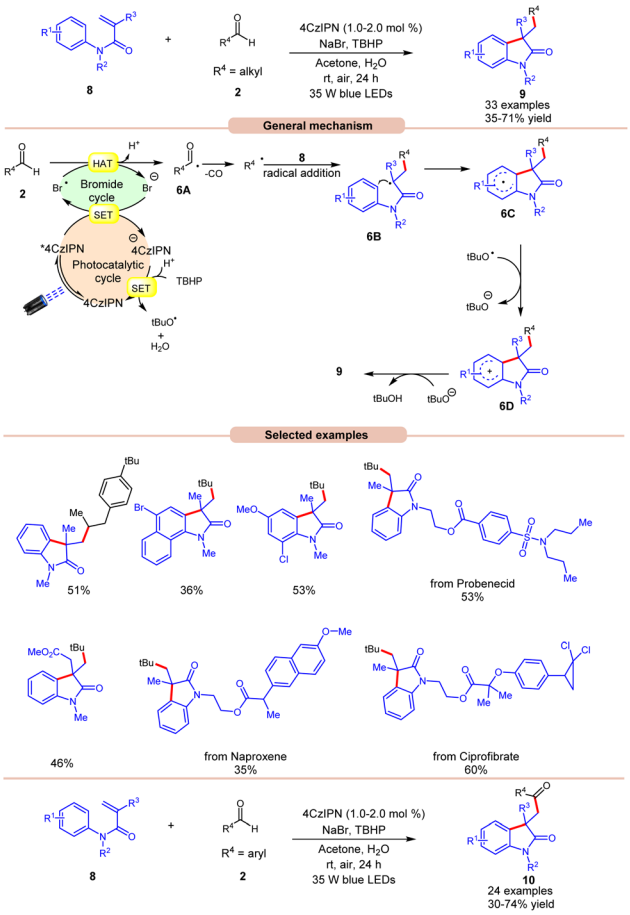

Scheme 6 4CzIPN-catalyzed radical acylation of *N*-arylacrylamides with aliphatic or aromatic aldehydes.

N-arylacrylamides **8**, accompanied by cyclization to give access to radical intermediate **6C**. Lastly, the SET/deprotonation of **6C** yields the required alkylated product **9**. Furthermore, under similar photocatalytic conditions, the authors demonstrated the acylation of *N*-arylacrylamides **8** using aromatic aldehydes **2** to afford the required acylated products **10**. Notably, replacing aliphatic aldehydes with aromatic aldehydes under the same optimized conditions provides the acyl-substituted oxindoles **10** in 30–74% yields. Probably secondary and tertiary aliphatic aldehydes undergo decarbonylation due to the formation of stable alkyl radicals.

A highly effective approach towards the hydroacylation of vinyl arenes **11** was accomplished by Wu and co-workers using *N*-bromosuccinimide (NBS) as a catalyst under visible light irradiation (Scheme 7a).[16a] The striking feature of this protocol is that it does not require any external photocatalyst to generate the bromine radical. The ideal reaction conditions comprised NBS in fluorobenzene at 80 °C under blue light irradiation. Notably, the application of a non-aromatic solvent in the reaction mixture failed to give the targeted product. A broad range of styrene derivatives **11** reacted well with alkyl and aryl aldehydes **2**, affording the hydroacylated product **12** in 32–75% yield. A TEMPO trapping experiment inhibited the product formation,

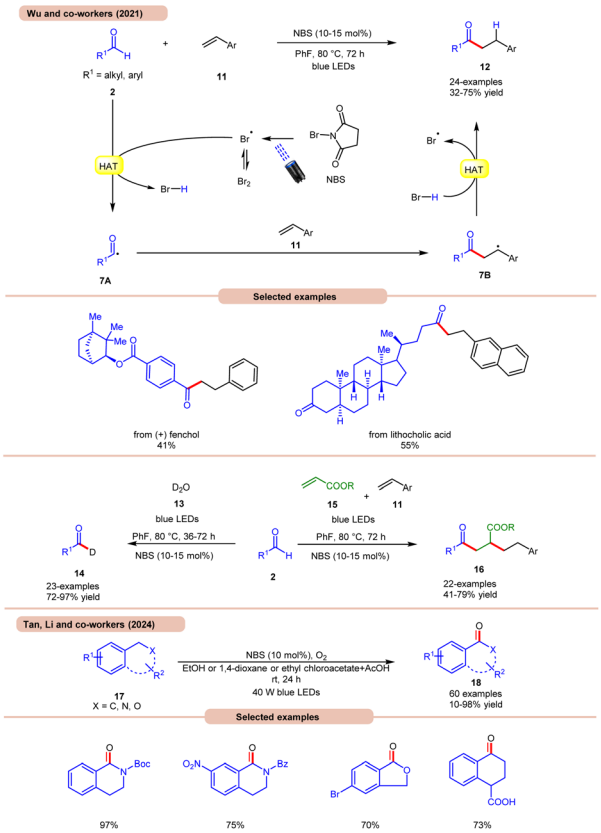

Scheme 7 Bromine-radical catalyzed hydroacylation of vinyl arenes.

indicating a radical mechanistic pathway. Light on/off studies indicated that visible light irradiation is crucial for the homolysis process. As shown in Scheme 7, in the presence of visible light irradiation, NBS undergoes N–Br bond homolysis to give a bromine radical in equilibrium with molecular bromine. Subsequently, the aldehyde group **2** undergoes HAT with the bromine radical to give HBr and acyl radical intermediate **7A**, which adds to the terminal alkene position to give a benzyl radical intermediate **7B**. Lastly, the desired product **12** is obtained *via* HAT with HBr. Product formation was further supported by DFT calculations. This strategy could also be applicable to the deuteration of aldehydes **2** with D_2O **13**, affording the deuterated product **14** in 72–97% yield. The compatibility of this protocol was further seen in the radical cascade reaction involving acrylates **15** and styrene **11**, giving the desired product **16** in 41–79% yield.

Most recently, Tan, Li, and co-workers developed a metal-free photocatalytic system for aerobic oxygenation of the benzylic C(sp^3)–H bonds of amines, ethers, alkylarenes, and hetero-aromatics **17** (Scheme 7b).[16b] In this method, the authors employed readily available NBS as a bromine radical source and O_2 as an oxidant. The method has been successfully applied to the synthesis of bioactive and drug-valued targets, including corydaldine, ketoprofen, and isoflavone, providing good opportunities for applications in drug discovery and development.

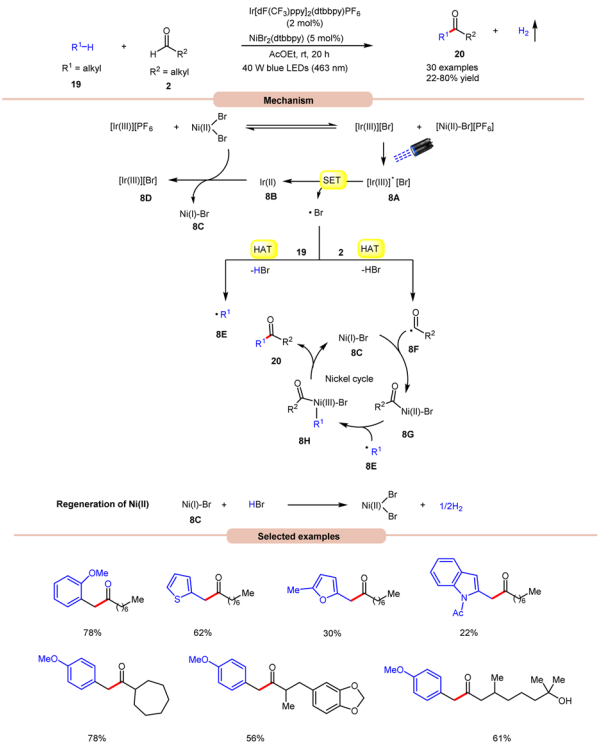

Scheme 8 Bromine radical-mediated dehydrogenative coupling reaction for the synthesis of aryl ketones.

Impressively, a new methodology for the synthesis of ketones **20** was developed by Kawasaki, Ishida, and Murakami, in 2020, by using a dual Ir-photoredox/nickel catalytic system (Scheme 8).[17] In this strategy, $NiBr_2$(dtbbpy) plays a dual role in the generation of a bromine radical and in the cross-coupling of benzylic and acyl radical intermediates. A variety of alkylarenes **19** were well tolerated with alkyl aldehydes **2** under the optimized conditions to yield the corresponding ketones **20** in 22–80% yields. A TEMPO trapping experiment supported the formation of benzylic and acyl radical intermediates. Mechanistically, an anion exchange interaction between Ir-photoredox and $NiBr_2$(dtbbpy) catalytic systems gives [Ir(III)][Br]-complex **8A**, which in the presence of visible light irradiation gives access to a bromine radical and Ir(II)-complex **8B** *via* a SET event between photoexcited [Ir(III)]* and bromide anions.

Subsequently, the bromine radical participates in a HAT reaction with the aldehyde **2** and benzylic **19** C–H bond to give acyl radical intermediate **8F** and benzylic radical intermediate **8E** along with HBr. The resulting acyl radical intermediate **8F** interacts with Ni(I)Br-species **8C** to give access to Ni(II)–Br species **8G**. Next, Ni(II)–Br species **8G** interacts with benzylic radical intermediate **8E** to give Ni(III)–Br complex **8H**. Lastly, reductive elimination generates the final product **20** with the regeneration of **8C**. Moreover, the interaction between **8C** and HBr regenerates the corresponding Ni-catalyst along with H_2. Notably, benzaldehydes did not yield successful outcomes in this protocol, primarily due to the challenge in abstracting the aldehydic hydrogen. This difficulty arises from the electron-withdrawing nature of the phenyl group attached to the aldehyde.

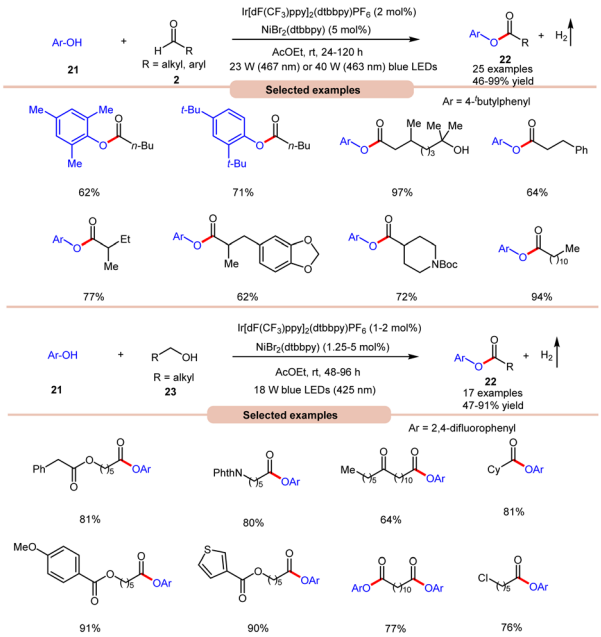

Scheme 9 Bromine radical-mediated acylation of phenol with aldehydes and alcohols.

With a slight change in the optimized conditions, the same group later reported a visible light-mediated acylation of phenols **21** with aldehydes **2** for the synthesis of esters **22** in a dual Ir-photoredox/nickel bromide catalytic system (Scheme 9a).[18a] A broad range of aromatic phenols **21** and alkyl and aryl aldehydes **2** reacted well to afford the corresponding esters **22** in 46–99% yield. The robustness of this protocol made it compatible with naturally occurring phenols such as β-arbutin and α-tocopherol. In continuation of their work, the same group later reported the acylation of phenols **21** using alkyl alcohols **23** to afford the required acylated products **22** in 47–91% yields under similar reaction conditions (Scheme 9b).[18b]

3. Hydrogen atom transfer from benzylic carbons

Hydrogen atom transfer (HAT) from a benzylic carbon refers to the abstraction of a hydrogen atom bonded to a carbon atom adjacent to a benzene ring. When a bromine radical species interacts with a substrate containing a benzylic carbon, it can abstract a hydrogen atom from this position, leading to the formation of a benzylic radical intermediate. Notably, benzylic hydrogen atoms are more readily abstracted in comparison to other hydrogen atoms in a molecule due to the stability of the resulting benzylic radical, which is resonance-stabilized by the delocalization of the unpaired electron into the aromatic ring (Scheme 10).

In this regard, an aerobic cross-dehydrogenative coupling (CDC) reaction was achieved by Huang, Deng, and co-workers in 2021 by a reaction between quinolines **1** derivatives and toluene **24** under visible light irradiation (Scheme 11).[19] Initial investigations were carried out on *p*-xylene and 4-methylquinoline as

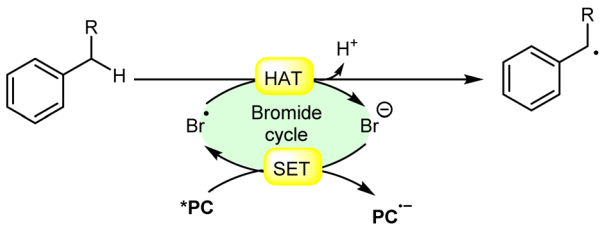

Scheme 10 General approach for benzyl radical intermediate formation *via* bromine radical-mediated HAT.

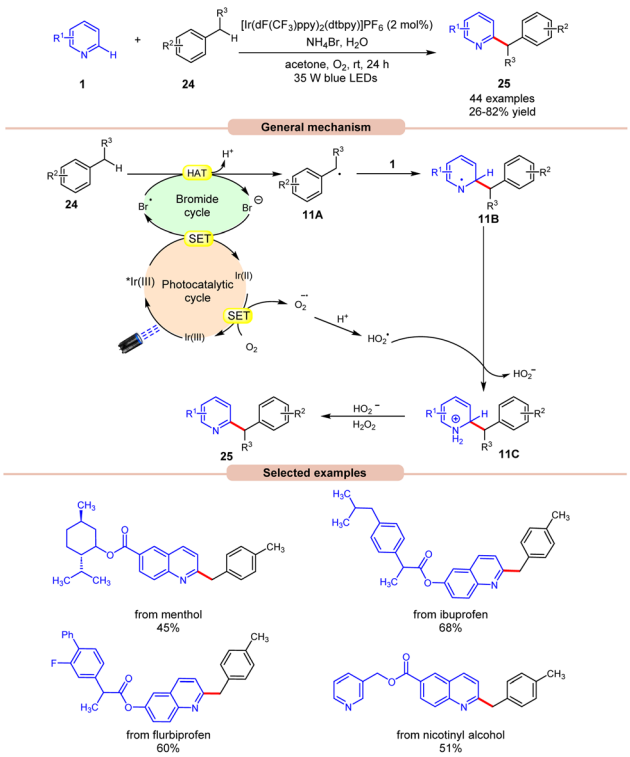

Scheme 11 Dual Ir-photoredox/NH_4Br catalyzed cross-dehydrogenative coupling of *N*-heteroarenes with toluenes.

model substrates for this Minisci-type CDC reaction. Optimized conditions revealed that light irradiation, a photocatalyst, and a bromide source are crucial for the transformation of this reaction. Out of the various bromide additives screened, NH_4Br as a bromide source displayed the highest efficiency in reaction yield. A library of substituted quinoline derivatives **1** with electron-donating and withdrawing functionalities reacted well with toluene under the optimized conditions to afford the desired products **25** in 26–82% yield. Notably, toluene derivatives **24** bearing electron-donating groups gave a higher product yield in comparison to those with electron-donating ones. Besides, ethylbenzene and 2-methylnaphthalene also worked well to afford the desired product in 33–45% yield. A radical trapping experiment with TEMPO and 1,1-diphenylethylene supported the involvement of a radical mechanistic pathway. A quantum yield experiment ($\Phi = 0.52$) eliminated the possibility of the radical chain pathway. As shown in Scheme 11, the photoexcited catalyst undergoes SET with the bromide anion to form a bromine radical, which undergoes HAT with the toluene **24** to form a benzyl radical intermediate **11A.** This intermediate adds to the quinoline **1** to form an *N*-centered radical intermediate **11B.** Subsequently, the oxidized catalyst Ir(II) is reduced by oxygen (O_2) to form a superoxide radical ($HO_2^{\bullet}$) along with the completion of the catalytic cycle. This superoxide radical ($HO_2^{\bullet}$) oxidizes the radical intermediate **11B** to generate a cation intermediate **11C**, which finally upon deprotonation yields the desired product **25.** The compatibility of this strategy was further demonstrated in the late-stage functionalization of biologically active molecules.

The following year, Liu, Feng and co-workers reported bromine radical-mediated enantioselective photoreduction of ketones **26** and hydrocarbons **19** for the synthesis of tertiary alcohols **27** (Scheme 12).[20] Both electron-rich and electron-withdrawing groups on pyridine-based ketones **26** were converted into tertiary alcohols in good yields. However, *ortho*-substituted diarylketones gave a lower yield than the *meta*- and *para*-substituted ones, probably due to steric hindrance. Moreover, allylic and saturated cyclic hydrocarbons gave the required products **27** in good yields and enantioselectivity. Mechanistically, it is proposed that the photoexcited *Ir(III) undergoes SET with the bromide ion, generating the bromine radical along with Ir(II). This bromine radical participates in HAT with the benzylic C(sp^3)–H partner **19**, producing an alkyl radical intermediate 12A. Next, the pyridine-based ketones **26** coordinate with the chiral Er(III)-complex to generate the complex 12B. Therefore, the complex 12B undergoes spatial-selective radical addition with the alkyl radical 12A, generating the chiral radical intermediate 12C. Lastly, the resulting radical intermediate 12C

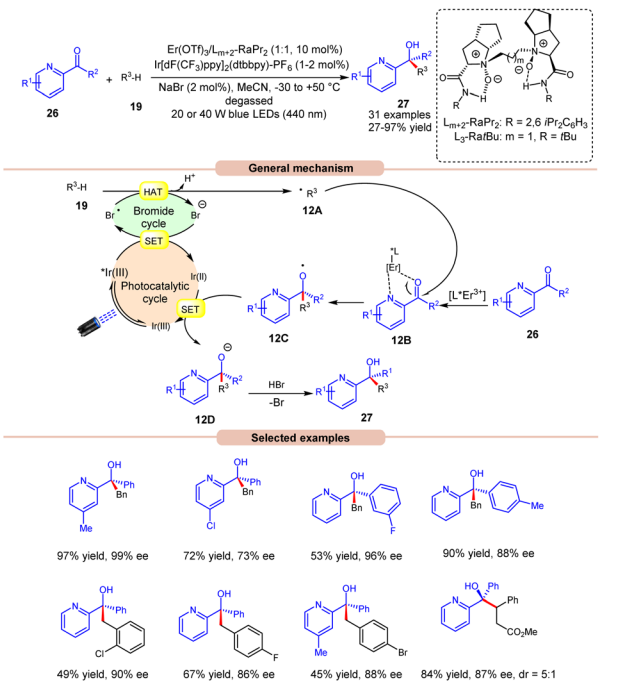

Scheme 12 Bromine radical enhanced photoreduction of ketones and hydrocarbons for synthesizing tertiary alcohols.

undergoes SET/protonation to access the desired tertiary alcohols 27 with bromide ions, which again initiate the catalytic cycle.

Recently, Deng and co-workers established visible light-induced benzylic C(sp^3)–H functionalization of petroleum-derived alkylarenes **24** with trifluoromethyl ketones **28** to give trifluoromethyl alcohols **29** (Scheme 13).[21] Substituted toluenes **24** with electron-donating and electron-withdrawing groups at various positions were well tolerated, accessing the desired products **29** in 42–82% yields. Furthermore, the *meta*- and *ortho*-substituted toluenes **24** gave the required products **29** in relatively low yields. In addition, methyl heteroarenes such as 2-thienyl, 2-furyl, and 2-methylnaphthalene reacted smoothly and gave the corresponding products in moderate yields. The robustness of this protocol is further demonstrated by the late-stage functionalization of complex bioactive molecules such as isoxepac, ciprofibrate, ibuprofen, flurbiprofen, ketoprofen, and naproxen. Radical trapping experiments using TEMPO, BHT and hydroquinone suggest the involvement of a radical pathway. Mechanistically, the photoexcited *Ir(III) complex oxidizes the bromine anion to generate the bromine radical, which abstracts a hydrogen atom in alkylarenes **24** to give benzyl radical **13A**. Next, trifluoromethyl ketones **28** undergo a proton-coupled electron transfer (PCET) process with the reducing Ir(II)-complex to give the ketyl intermediate **13B**. Finally, radical–radical coupling between the benzyl radical **13A** and ketyl intermediate **13B** affords the final desired product **29**.

In 2022, Huang, Deng and co-workers revealed a dual photoredox/nickel-catalyzed coupling of methyl arenes **24** with acid chlorides **30** *via* a bromine radical enhanced HAT pathway (Scheme 14).[22] The authors utilized an Ir-complex photocatalyst with $NiBr_2$ as a co-catalyst and bromine radical source in acetone. In this protocol, acid chloride **30** with electron-rich groups delivered better yields than the ones having electron-deficient groups.

Unfortunately, 4-nitro benzoyl chloride did not work in this reaction. In the case of methylarenes, *para*-substituted derivatives displayed better reactivity compared to *meta*- and *ortho*-substituted derivatives due to steric hindrance. The compatibility of this method was demonstrated in the late-stage functionalities of complex drug molecules such as ioxoprofen, ketoprofen, and flurbiprofen, *etc.* Radical trapping experiments suggested the involvement of a radical pathway and their trapped adduct confirmed the formation of an acyl radical. The authors proposed that reductive quenching of the photoexcited *Ir(III) catalyst with bromine anions generates Ir(II) and bromine radicals. Simultaneously, Ni(I) species were generated by the interaction between Ir(II) and Ni(II) species, which react with acid chlorides **30** to give acyl radical intermediate **14C** *via* intermediate **14D**. In turn, the methyl arene **24** undergoes HAT with the generated bromine radical to give radical intermediate **14A**, which upon oxidative addition with Ni(I) species generates Ni(II) intermediate **14B**. Lastly, the trapping of acyl radical **14C** and Ni(II) intermediate **14B**, followed by reductive elimination, yields the final product **31**. With a change in reaction conditions, the authors demonstrated the utility of this method in the acylation of methyl arenes **24** using alkyl acid chlorides **30** in good yields.

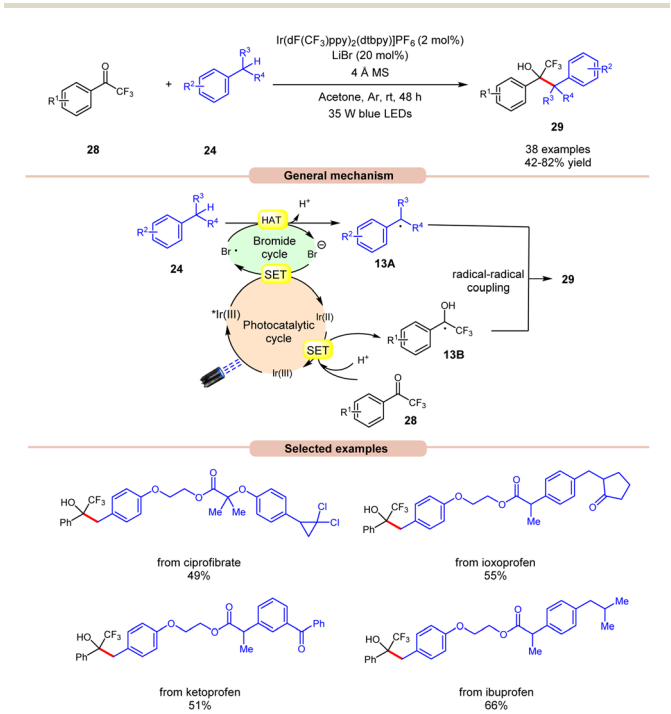

Scheme 13 Ir-catalyzed benzylic C(sp^3)–H functionalization of alkylarenes with trifluoromethyl ketones.

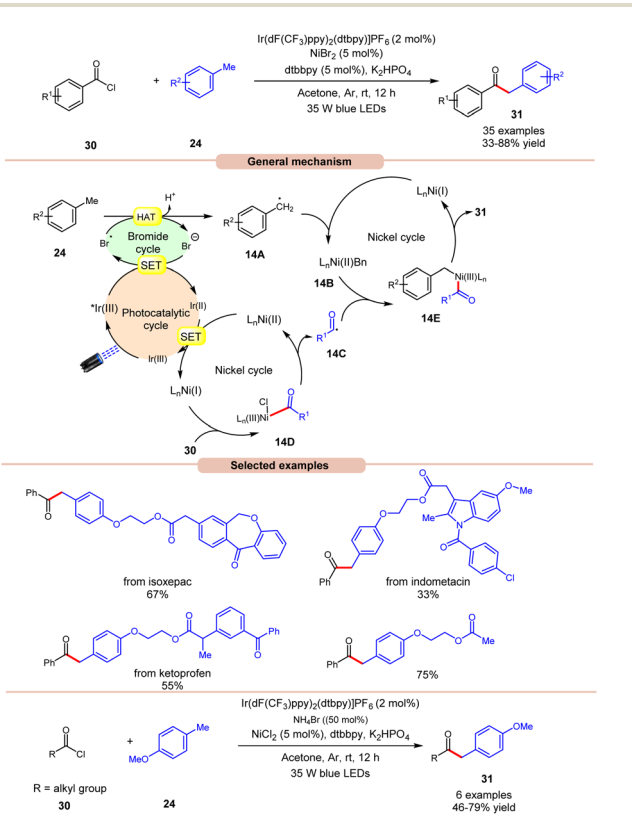

Scheme 14 Dual Ir/nickel-catalyzed coupling of methyl arenes with acid chlorides.

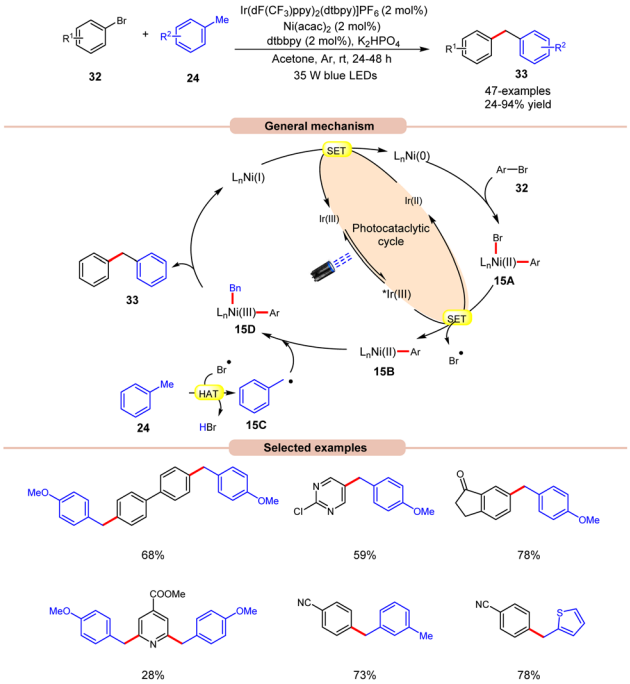

Scheme 15 Dual Ir/Ni-catalyzed arylation of the benzylic C–H bonds of toluene derivatives with aryl bromides.

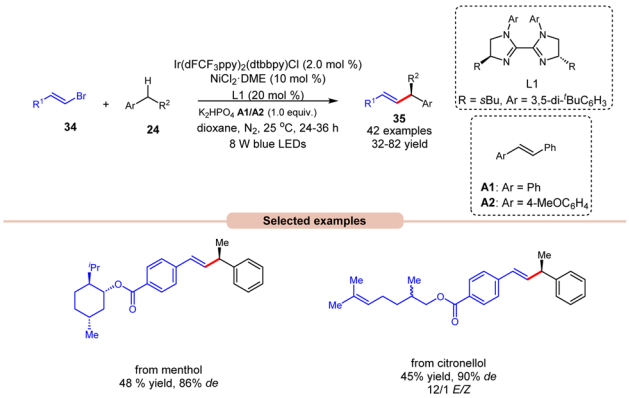

Scheme 16 Dual Ir/nickel-catalyzed synthesis for stereo- and enantio-selective benzylic C(sp^3)–H alkenylation.

In 2022, Deng and co-workers reported dual Ir/Ni-catalyzed arylation of benzylic C–H bonds of toluene derivatives **24** with aryl bromides **32** (Scheme 15).[23] Here, cross-coupling reactions were successfully conducted with a wide range of aryl- and heteroaryl bromides **32** containing electron-deficient, neutral, or electron-donating functional groups. It was further observed that substrates with electron-rich groups resulted in reduced yields of the corresponding coupling products **33**. Mechanistically, the Ni(II) aryl bromide intermediate **15A** was generated through the oxidative addition of the Ni(0) complex to aryl bromide **32**. Next, the photoexcited *Ir(III) undergoes SET with **15A** to give an aryl Ni(II)-species **15B** and bromine radical (Br$^{\bullet}$). This bromine radical abstracts the hydrogen atom from toluene derivative **24**, to produce benzyl radical **15C**. Following this, the Ni(II) aryl species **15B** reacts with the benzylic radical **15C**, yielding the Ni(III) aryl alkyl species **15D**. Moreover, upon reductive elimination, the desired 1,1-diaryl alkane **33** is formed with the generation of the Ni(I) species, which transforms into the Ni(0) species *via* SET with the Ir(II) complex, thus concluding both catalytic cycles. The synthetic versatility of this method was further demonstrated in the late-stage arylation or benzylation of numerous drug-like and complex molecules.

Alkenylation reactions are versatile tools in organic synthesis, enabling the formation of carbon–carbon double bonds with high efficiency and selectivity. They find wide application in the preparation of pharmaceuticals, agrochemicals, and materials science.[24] In this context, Lu and coworkers demonstrated stereo- and enantio-selective benzylic C(sp^3)–H alkenylation, using a dual Ir/nickel catalytic system for the synthesis of chiral allylic compounds **35** (Scheme 16).[25] Easily accessible alkylbenzenes **24** and alkenyl bromides **34**, including complex molecules, participated in this cross-coupling reaction to afford the desired allylic compounds **35** with up to 93% ee and a >20/1 *E*/*Z* ratio under mild reaction conditions with good functional group tolerance. Alkenyl bromides **34** with electron-rich or electron-deficient aryl substituents were well tolerated. It is crucial to underscore the significance of stilbene as an additive since it acts as a triplet energy transfer inhibitor. This function effectively blocks the direct energy transfer event from the excited state photocatalyst to the product and eliminates the isomerization of the double bond. Furthermore, this methodology has been effectively utilized in bromides derived from natural products, affording the desired products **35** in moderate yields. The mechanism for product formation occurs in the manner as discussed in previous Scheme 15.

An unprecedented approach towards the selective alkylation of unactivated C(sp^3)–H bonds **19** was achieved by Wu and coworkers in 2020, using a stop-flow micro-tubing reactor (SFMT) under visible light irradiation (Scheme 17).[26] The authors observed that the utilization of CH_2Br_2 as a solvent, as well as a bromine radical source, was best suited for this alkylation reaction of the tertiary unactivated C(sp^3)–H **19** bond by using a metal-free acridinium catalyst (Mer-AcrClO$_4$). A series of tertiary alkanes **19** bearing electron-donating and electron-withdrawing alkyl and aryl groups reacted well, affording the corresponding products **37** in 41–95% yields. This reaction also achieved higher reactivity when conducted under flow microtubing reactors, compared to batch reactors. The screening of different photocatalysts revealed that Mer-AcrClO$_4$ is highly reactive in catalyzing the reaction and a bromine radical could be effectively generated from CH_2Br_2 under photocatalytic conditions. Mechanistically, the photoexcited catalyst oxidizes CH_2Br_2, which eventually gives a bromine radical. Furthermore, the tertiary alkyl group **19** undergoes HAT with the bromine radical to give a radical intermediate **17A**. This intermediate interacts with the Michael acceptor **36** to give radical intermediate **17B**, accompanied by SET/protonation to yield the final product **37**. Moreover, this technology was also applied in the amination of C(sp^3)–H bonds **19** using dialkyl azodicarboxylates **38** as an aminating reagent, affording the corresponding products **39** in 49–78% yield. Notably, this method worked well

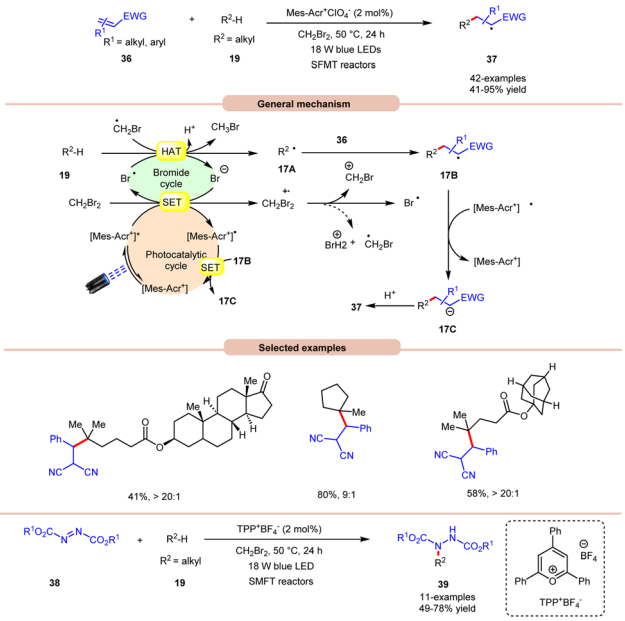

Scheme 17 Bromine radical-assisted alkylation and amination of C(sp^3)–H bonds.

with secondary and tertiary unactivated alkyl groups, whereas it failed with primary alkyl groups due to the lower stability of the alkyl radical.

4. Hydrogen atom transfer from α-heterocarbons

Hydrogen atom transfer (HAT) involving an α-heteroatom refers to the abstraction of a hydrogen atom bonded to a carbon atom adjacent to a heteroatom (such as nitrogen, oxygen, sulfur, *etc.*). This type of reaction commonly occurs in organic chemistry and plays a significant role in various chemical transformations. In a molecule containing an α-heteroatom, the heteroatom can influence the reactivity of the adjacent carbon–hydrogen bonds. The electronegativity or the presence of lone pairs on the heteroatom can affect the bond strength and polarity of the adjacent C–H bond, making it more susceptible to abstraction by the bromine radical (Br$^\bullet$) (Scheme 18).

In 2019, Huang and co-workers reported visible light Ir-photoredox catalyzed Minisci-type alkylation of quinolines **1** with ethers **40** serving as the alkylating agents (Scheme 19).[27]

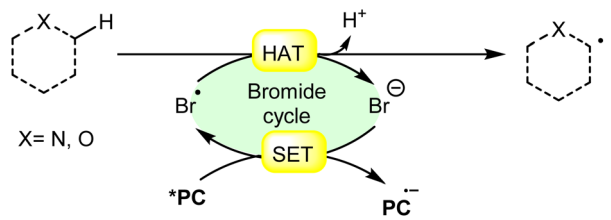

Scheme 18 General approach for α-heteroatom radical intermediate formation *via* bromine radical-mediated HAT.

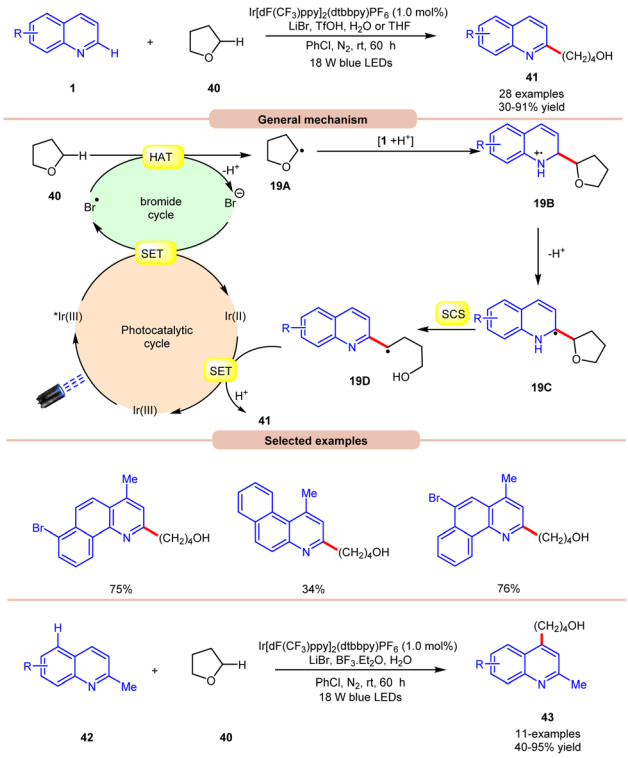

Scheme 19 Ir-photoredox catalyzed Minisci-type alkylation of quinolines with ethers.

The reaction demonstrates a wide range of functional group compatibility for both C_2 and C_4 coupling/alkylation of quinolines **1**. Notably, the C-4 substituted and unsubstituted quinolines and benzoquinolines provided the desired C-2 alkylated products **41** in 30–91% yields.

A radical trapping experiment with TEMPO supports the involvement of a radical pathway. Mechanistically, the generated bromine radical (Br$^\bullet$) abstracts a hydrogen atom from THF **40**, resulting in the generation of an alkyl radical **19A**, which adds to the charged compound **1**, leading to the formation of the radical cation **19B**. Subsequently, the radical cation **19B** undergoes deprotonation, followed by a spin-centre shift (SCS) process to ultimately give rise to an alkyl radical intermediate **19D** *via* C–O bond cleavage. Conclusively, the SET/protonation of **19D** ultimately yields the desired alkylated quinoline product **41**, while simultaneously regenerating the Ir(III) species.

In this work, an extension of C-2 blocked quinoline **42** gave the C-4 alkylated quinolines **43** in 40–95% yield by replacing TfOH with the Lewis acid $BF_3 \cdot Et_2O$. The substrate scope revealed that 2-methylquinolines **42** with different functional groups were smoothly reacted to give the C-4 alkylated product **43**.

On the other hand, Deng and co-workers developed a visible-light Ir-photoredox catalyzed C(sp^3)–H monofluoroalkenylation of ethers **40** for the synthesis of multi-substituted monofluoroalkenes **45** *via* selective HAT and radical–radical cross-coupling (Scheme 20a).[28a] This reaction shows high regioselectivity for the α-carbon atoms of THF **40**, thus allowing the synthesis of monofluoroalkenes **45** in yields of up to 92%. The

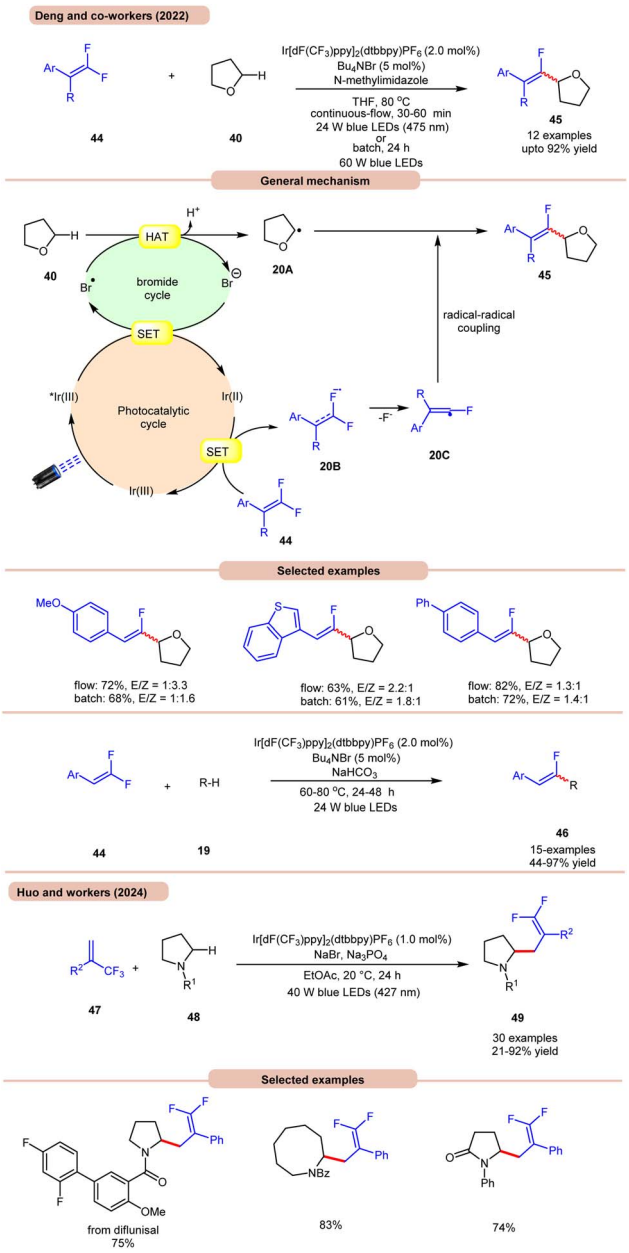

Scheme 20 Ir-photoredox catalyzed C(sp^3)–H monofluoroalkenylation of ethers.

substrate scope demonstrated a good functional group tolerance and could be carried out even on a gram scale.

Radical trapping experiments suggested that the reaction proceeds *via* a radical pathway. The TEMPO-THF adduct was further confirmed by GCMS and the 1,1-diphenylethylen-THF adduct was also isolated. As shown in Scheme 20, the key alkyl radical intermediate **20A** is formed *via* HAT between **40** and the bromine radical. At the same time, the fluoroalkenyl radical **20C** was generated *via* SET reduction of **44** by the Ir(II)-complex and cleavage of the C–F bond. Finally, targeted product **45** is generated by the radical–radical cross-coupling of **20A** and **20C**.

The authors also illustrated the monofluoroalkenylation of cyclic and acyclic ethers, aliphatic aldehydes, and amides **19** as substrates, to afford the desired products **46** in 44–97% yields. It is worth noting that in Scheme 19, ring-opening of THF occurs, while in Scheme 20a, no ring-opening occurs in the reaction medium. This is due to the use of triflic acid (TfOH) in the reaction mixture, while in the absence of TfOH, no C–O cleavage occurs.

Huo and co-workers in 2024 reported photoredox-catalyzed, bromine-radical-mediated C(sp^3)–H difluoroallylation of amides **48** (Scheme 20b).[28b] The authors used Ir[$dF(CF_3)ppy]_2$(dtbbpy)PF_6 as a photocatalyst, NaBr as a HAT reagent, and Na_3PO_4 as a base in EtOAc under blue LEDs. This method incorporates both acyclic and cyclic-amino C(sp^3)–H bonds **48** with a broad range of readily available trifluoromethyl alkenes **47**, providing difluoroallylated amine derivatives **49** in good to excellent yields.

Polychloromethylated hydrocarbons are omnipresent in various bioactive compounds and their synthesis has gained some attention in the scientific community.[29] In this regard, the synthesis of 1,1-dichloroalkane products **51** was achieved by Ji, Huang, and co-workers in 2022, using a dual Ir-photoredox/LiBr reaction system under visible light irradiation (Scheme 21).[30] Initial studies were carried out on *N*-phenylmethacrylamide **8** and chloroform **50** at room temperature. Out of the various bases screened, the application of Et_3N was proven to be highly efficient, affording the desired product **51** in 31–96% yield with H_2O as a proton source and LiBr as an additive. *N*-phenylmethacrylamide **8** bearing various functional groups at the *para*-position of the benzene ring reacted well with chloroform **50**, affording the targeted products **51** in 62–96% yield. On the other hand, α-naphthyl and β-naphthyl substituted

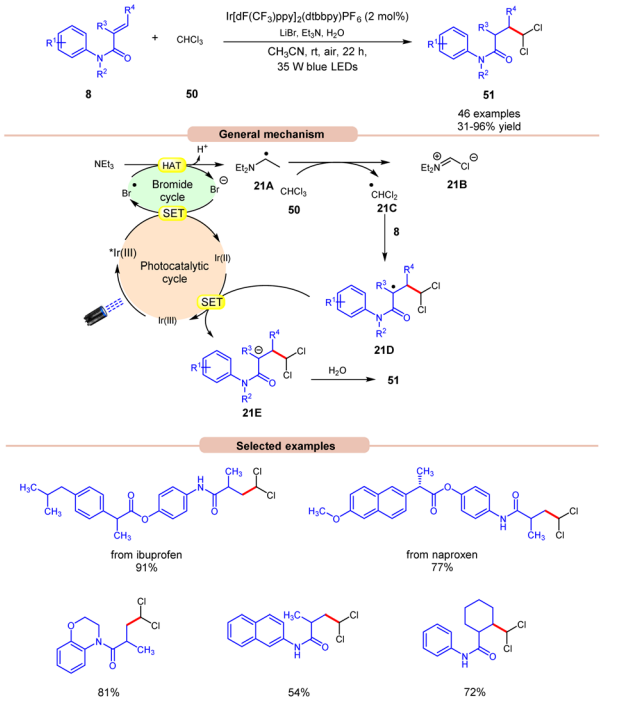

Scheme 21 Dual Ir-photoredox/LiBr catalyzed 1,1-dichloromethylation of alkenes using chloroform.

methylacrylamides **8** resulted in the targeted product in moderate yields (47–54% yield). Besides, *N*-phenylmethacrylamide **8** with internal and terminal alkenes smoothly reacted under the ideal conditions to yield the desired products in 39–86% yield. The compatibility of this reaction was further demonstrated in the late-stage functionalization of naproxen and ibuprofen derivatives, resulting in the desired dichloromethylated products **51** in 77% and 91% yields, respectively. The generation of the $^{\bullet}CHCl_2$ radical intermediate is confirmed by a radical trapping experiment with 1,1-diphenylethylene. Deuterated studies with D_2O supported the incorporation of a proton source from H_2O into the α-position of the carbonyl group of the dichloromethylated product. As shown in Scheme 21, the photoexcited catalyst *Ir(III) oxidizes the bromide anion to a bromine radical intermediate, which participates in HAT with Et_3N to give radical intermediate **21A**. This intermediate abstracts a chlorine atom from $CHCl_3$ to give the key $^{\bullet}CHCl_2$ radical intermediate **21C**, which adds to the terminal alkene **8** to give radical intermediate **21D**. Finally, the desired product **51** is obtained *via* SET/protonation.

Giedyk and co-workers, in 2020, reported facile Ir-photoredox catalyzed Minisci-type alkylation of *N*-heteroarenes **1** with non-activated alkyl bromides **52** as radical precursors (Scheme 22).[31] This photochemical system has proven to be robust and versatile, accommodating a wide range of primary and secondary alkyl bromides **52** with a variety of *N*-heterocycles **1**. Expectedly, secondary alkyl bromides **52** produced higher yields than primary ones, due to the higher thermodynamic stability of the radical intermediate. Under the optimized conditions, the photocatalyst *Ir(III) oxidizes the bromide ion to generate a bromine radical and Ir(II). This Ir(II) complex subsequentially absorbs a second photon, leading to the generation of a highly reducing state of the Ir complex *Ir(II). Next, the *Ir(II) complex undergoes a SET event with alkyl bromide **52,** followed by fragmentation forming an alkyl radical **22A** and bromide anion, which participates in the catalytic cycle. The resulting alkyl radical **22A** adds to the *N*-heteroarenes **1**, followed by HAT with the bromine radical, which leads to the formation of the cation intermediate **22C**. Finally, the desired product **53** is obtained *via* work-up. Moreover, the authors demonstrated the C–H alkylation of heteroarene **1** by using cetyl trimethyl ammonium bromide (CTAB) as a cationic surfactant with NaBr in the reaction medium to give the desired product **53** in 39–92% yield. It is worth noting that the reaction worked well with primary alkyls containing free hydroxy, chloride, amide, and $-CF_3$ groups. Unfortunately, alkyl bromides bearing acetal groups remained inactive in this protocol.

A visible light-mediated dual Ni/organophotoredox catalyzed C(sp^3)–H cross-coupling reaction with aryl bromide **52** was disclosed by König and co-workers in 2020, using NaBr as a bromide source (Scheme 23).[32] A variety of linear and branched alkyl bromides **52** reacted well with the cyclic ether to afford the C(sp^3)–H cross-coupling products **55** in moderate to good yields. Interestingly, benzyl chloride was also found to be an excellent coupling partner for this transformation. Moreover, the reaction could also be conducted on a gram scale. Based on previous reports, the authors postulated that the oxidative addition of Ni(0) into an aryl bromide **52** produces Ni(II) aryl bromide intermediate **23A**. Next, the photoexcited catalyst 4CzIPN* oxidizes **23A** to produce Ni(III) intermediate **23B**. The photolysis of **23B** results in the generation of

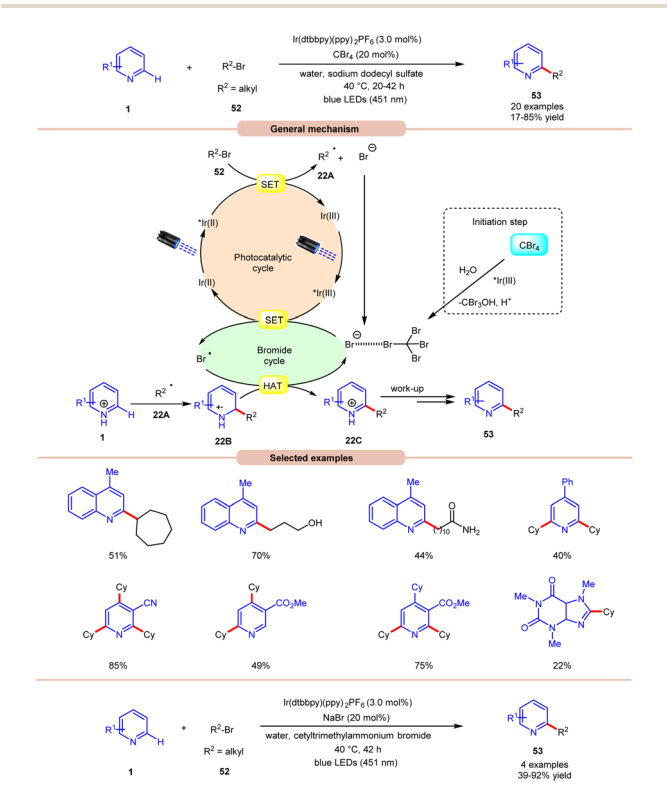

Scheme 22 Ir-photoredox catalyzed Minisci-type alkylation of *N*-heteroarenes with non-activated alkyl bromides.

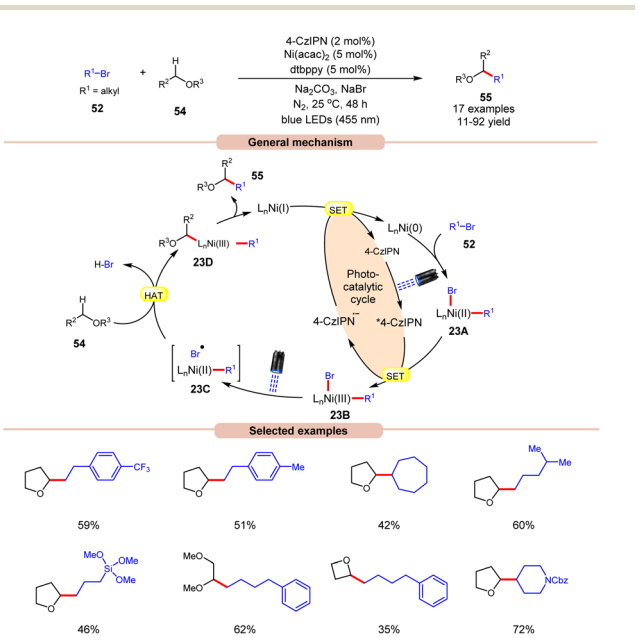

Scheme 23 Dual Ni/organophotoredox catalyzed C(sp^3)–H cross-coupling reaction with aryl bromide.

a bromine radical and Ni(II) species **23C**. The resulting bromine radical rapidly abstracts a hydrogen atom from α-carbon to oxygen, resulting in a C-centered radical intermediate, which adds to the Ni(II)-complex to produce Ni(III) species **23D**. Subsequently, reductive elimination yields the desired C(sp^3)–H cross-coupling product **55**. Lastly, the SET reduction of the resulting Ni(I) intermediate by the highly reducing 4-CzIPN$^{\bullet-}$ species regenerates the Ni(0)-complex, thus completing the catalytic cycle.

In 2022, Song and co-workers reported visible light-mediated direct C–H difluoroalkylation of quinoxalinones **56** with bromodifluoroacylarenes **57** *via* C(sp^3)–Br bond homolytic cleavage (Scheme 24a).[33a] In this method, quinoxalin-2(1*H*)-ones **56** bearing electron-rich or electron-deficient functionalities readily afforded the desired difluoroalkylated products **58** in 30–87% yields. Several control experiments were performed to determine the reaction mechanism. Under visible light irradiation, the C(sp^3)–Br bond undergoes homolysis to generate a difluoroalkyl radical intermediate **24A**, which was further supposed by radical trapping experiments, and their adducts were confirmed by using HRMS analysis. Mechanistically, visible light-promoted C(sp^3)–Br bond homolysis from $ArCOCF_2Br$ **57** generated the difluoroalkyl radical intermediate **24A** and bromine radical. The bromine radical abstracts the hydrogen atom from quinoxalinone **56** to produce radical intermediate **24B** with the release of HBr. The generated radical intermediate **24B** undergoes radical coupling with difluoroalkyl radical **24A** to furnish the desired products **58**. The authors further expanded their work to the C(sp^2)–H functionalization of aldehyde-derived hydrazones **59** with bromodifluoroacylarenes **57** for the direct preparation of functionalized α-iminodifluoroalkylated products **60**. The substrate scope revealed that a variety of (hetero)aryl aldehyde-derived hydrazones **59** bearing either electron-rich or electron-deficient groups were efficiently transformed into the required products **60** with good to excellent yields. In this protocol, unsaturated aldehyde-derived hydrazones **59** such as alkynals, alkenals, and ester aldehydes were also compatible to obtain a series of complex difluoroalkylated products **60**.

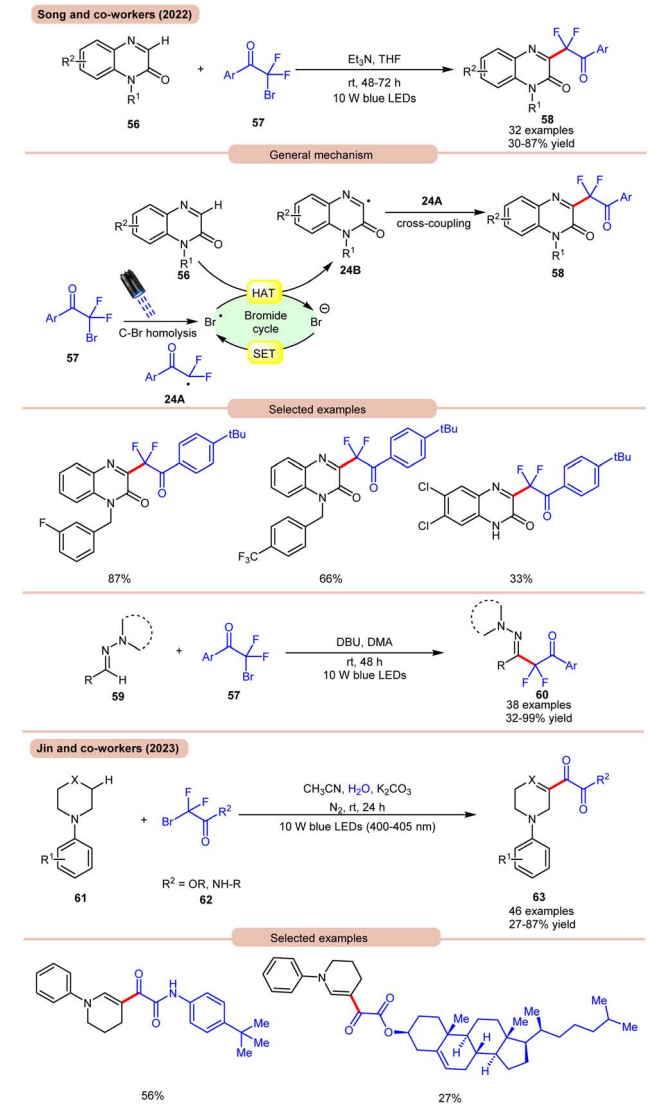

Scheme 24 Visible light mediated direct C–H difluoroalkylation of quinoxalinones with bromodifluoroacylarenes.

On the other hand, using difluoromethyl bromide **62** and H_2O, Jin and co-workers in 2023 reported the β-alkoxyoxalylation of *N*-aryl cyclic amines **61** for the synthesis of β-ketoester/ketoamide substituted enamines **63** in 27–87% yields (Scheme 24b).[33b] It was proposed that difluoromethyl bromide undergoes homolysis to give a bromine radical, which participates in HAT and gives the key difluoroalkylated intermediate. This intermediate further reacts in the presence of H_2O to give the desired product **63**. In 2021, Huang and co-workers disclosed a visible light-mediated photoredox Minisci alkylation reaction of 4-hydroxyquinazolines **65** with ethyl acetate **64** (Scheme 25).[34] In this protocol,4-hydroxyquinazolines **65** bearing various electron-donating and electron-withdrawing functionalities reacted well with ethyl acetate **64** to afford the desired products **66**.

Other alkylating reagents **64** such as isobutyl acetate, isopropyl acetate, *n*-pentyl acetate, *n*-butyl acetate, and *n*-heptyl acetate were also well tolerated, affording the required product **66** in low to moderate yields (18–55%). The reaction was completely suppressed in the presence of TEMPO, BHT, and DPE, which supported the involvement of a radical mechanistic pathway. Mechanistically, the photoexcited catalyst *Ir(III) is reduced by the bromide ion, leading to the generation of a bromine radical (Br$^{\bullet}$). The bromine radical then initiates the abstraction of a hydrogen atom from ethyl acetate **64**, resulting in the formation of an alkyl radical **25A**. This alkyl radical **25A** undergoes a radical addition reaction with 4-hydroxyquinazoline **65**, accompanied by deprotonation, leading to the formation of radical intermediate **25C**. Following this, a spin-center shift (SCS) process takes place, with the elimination of acetic acid (AcOH), resulting in the production of the radical intermediate **25D**. Finally, upon SET/protonation, the required alkylated product **66** is obtained. Simultaneously, this step regenerates the Ir(III) species, completing the catalytic cycle. The applicability of this method was further demonstrated in the

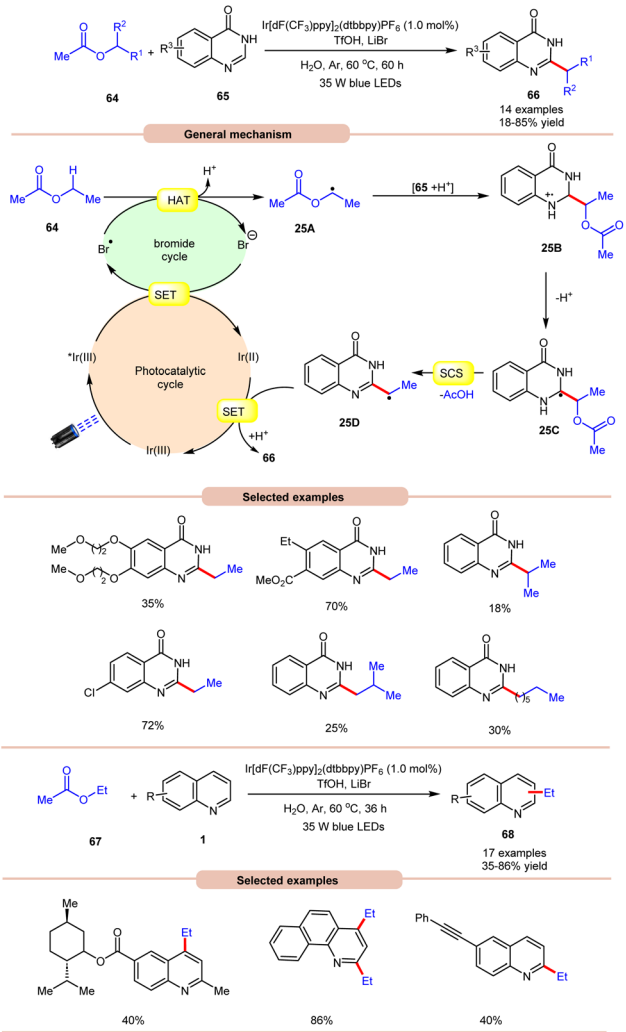

Scheme 25 Ir-catalyzed Minisci alkylation reaction of 4-hydroxyquinazolines with ethyl acetate.

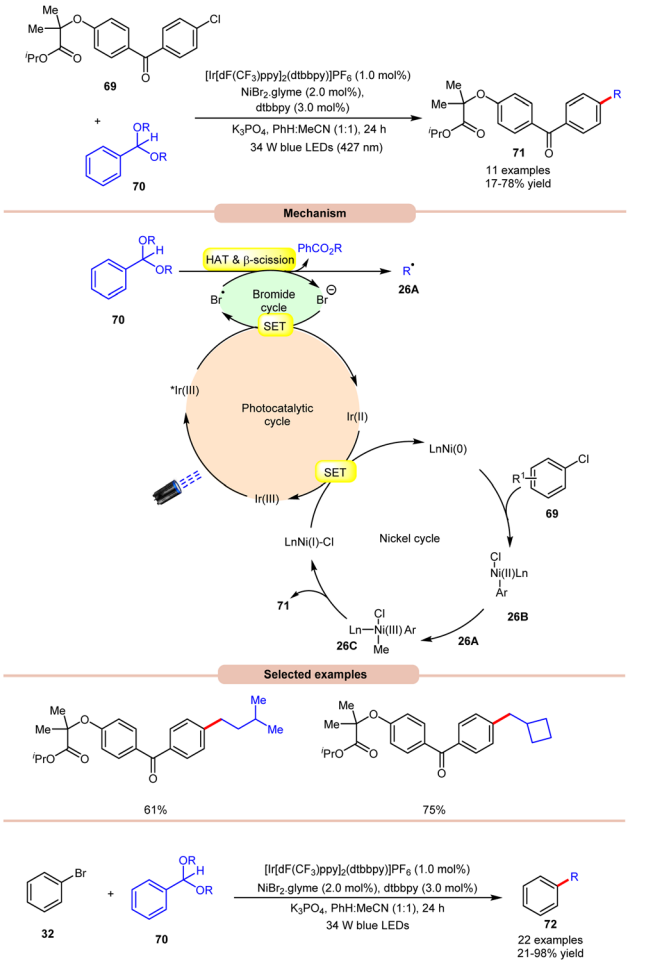

Scheme 26 Dual Ir/Ni-photoredox-catalyzed alkylation and (deutero) methylation of aryl halides.

alkylation of quinoline and pyridine **1** derivatives under the optimized conditions, giving the required product **68** in 35–86% yield.

Doyle and co-workers in 2022, reported a dual Ir/Ni-photoredox catalyzed alkylation and (deutero)methylation of aryl halides **69** by using benzaldehyde di(alkyl) acetals **70** (Scheme 26).[35] This protocol was found to be compatible with the late-stage functionalization of fenofibrate, which possesses an aryl chloride. The authors proposed that the photoexcited *Ir(III) oxidizes the bromide ion to a bromine radical, which undergoes HAT with the tertiary C–H bond of the acetal **70**, followed by β-scission to afford an alkyl radical **26A** and alkyl benzoate. Thereafter, the Ni(0)-complex undergoes oxidative addition with an aryl chloride and produces a Ni(II) aryl chloride intermediate **26B**. The alkyl radical **26A** is captured by **26B**, generating Ni(III)–(Ar)(Me) species **26C**, accompanied by reductive elimination to yield the desired product **71** and Ni(I)-complex. The reduced photocatalyst Ir(II) can then reduce Ni(I) to regenerate both Ir(III) and Ni(0)-catalysts. The authors further demonstrated the C(sp^2)–C(sp^3) cross-coupling reaction between acetals **70** as the source of aliphatic coupling partners with aryl bromides **32** to give the desired products **72** in 21–98% yield.

5. Hydrogen atom transfer from $(Me_3Si)_3SiH$

Hydrogen atom transfer (HAT) from $(Me_3Si)_3SiH$ (trimethylsilyl hydride) induced by a bromine radical is a well-known reaction in radical chemistry. Trimethylsilyl hydride is commonly used as a hydrogen atom donor in radical reactions due to its relatively weak Si–H bond and its ability to efficiently transfer a hydrogen atom to radical species. When a bromine radical encounters trimethylsilyl hydride, it can abstract a hydrogen atom from the Si–H bond, leading to the formation of a trimethylsilyl radical ($(Me_3Si)_3Si^{\bullet}$) and hydrogen bromide (HBr). This process can be represented by the following equation (Scheme 27):

The resulting trimethylsilyl radical can further participate in various radical reactions, such as radical chain reactions or radical-mediated functionalization reactions. This type of hydrogen atom transfer is widely utilized in organic synthesis for the generation of radicals and the construction of complex molecules.

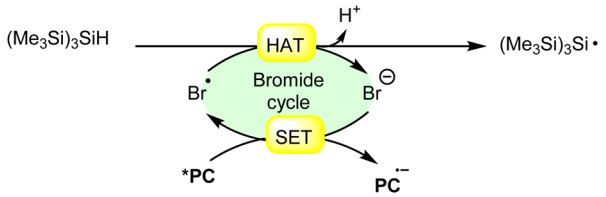

Scheme 27 General approach for trimethylsilyl radical intermediate formation *via* bromine radical-mediated HAT.

In 2018, ElMarrouni, Balsells and co-workers introduced a mild procedure for the direct visible light-initiated Giese addition of unactivated alkyl bromides **52** to electron-poor olefins (Michael acceptor) **73** or **74** (Scheme 28).[36] In this process, visible light prompts the generation of an alkyl radical as a crucial intermediate from unactivated alkyl halides. This $C(sp^3)$–$C(sp^3)$ bond formation proved to be highly efficient, accommodating a range of alkyl bromides successfully applied in the reaction of cyclic or acyclic α,β-unsaturated esters and amides. Mechanistic investigations suggested that the photo-excited *Ir(III) complex oxidizes the bromide ion to form a bromine radical, which abstracts a hydrogen atom from $(Me_3Si)_3SiH$ to generate stabilized silyl radical intermediate **28A.** This intermediate **28A** rapidly undergoes halogen atom abstraction with the alkyl bromide **52**, giving rise to the alkyl radical **28B** and a bromosilane by-product. The alkyl radical **28B** adds to the double bond of the Michael acceptor **73,** generating another carbon radical intermediate **28C.** A single-electron transfer (SET) between radical intermediate **28C** and the reductant species Ir(II) provides an anion intermediate **28D,** which upon protonation furnishes the desired product **75.** Alternatively, hydrogen atom abstraction from $(Me_3Si)_3SiH$ yields the corresponding product **75,** thereby regenerating stabilized silyl radical species **28A.** Notably, this methodology could be leveraged to access a key intermediate of vorinostat, an HDAC inhibitor employed in combating cancer and HIV.

In 2019, Wang and co-workers introduced an Ir-photoredox catalyzed Minisci C–H alkylation of heteroarenes **1** with unactivated primary, secondary, and tertiary alkyl bromides **52** by employing visible light irradiation (Scheme 29).[37] This method demonstrated the efficient incorporation of a diverse array of cyclic and acyclic, unactivated primary, secondary, and tertiary alkyl groups **52** into *N*-heteroarenes **1** under optimized reaction conditions. Impressively, the protocol exhibited scalability, successfully performing on a gram scale. Additionally, its robustness was demonstrated in the late-stage functionalization of complex *N*-containing natural products and drugs.

Lately, Zhao, Shi, and co-workers revealed bromine radical-mediated hydrosilylation of alkene **36** using $(TMS)_3SiH$ and $(n\text{-}Bu)_4NBr$ as HAT reagents (Scheme 30).[38] A wide range of electron-deficient alkenes and electron-rich alkenes **36** were reacted under this protocol to give the desired hydrosilylated products **78** in moderate to excellent yields. The compatibility of this method was further demonstrated in the late-stage functionalization of bioactive molecules in good yields.

MacMillan and co-workers, in 2016, developed a dual Ir/Ni-catalyzed approach towards the formation of a $C(sp^3)$–$C(sp^2)$

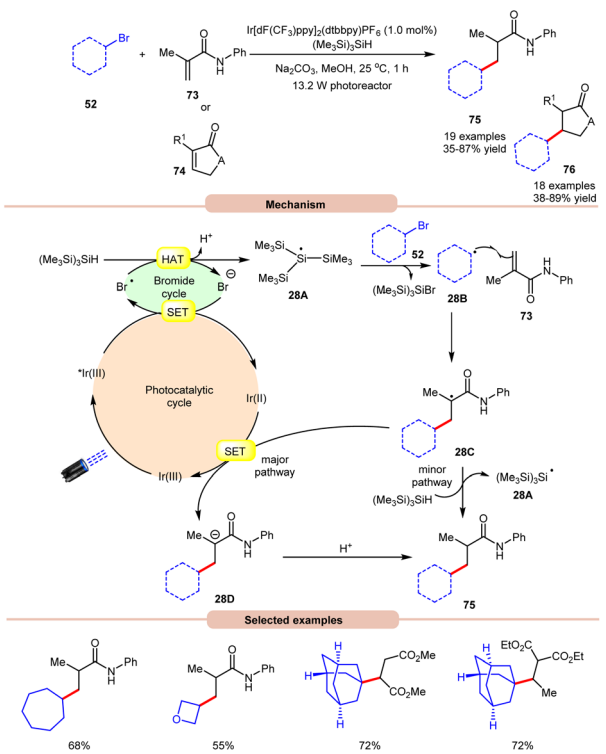

Scheme 28 Visible light-mediated Giese addition of unactivated alkyl bromides to electron-poor olefins.

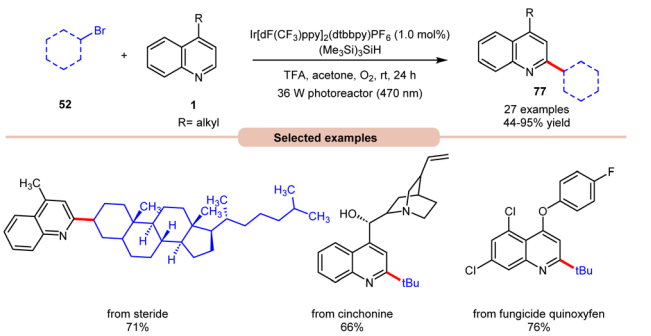

Scheme 29 Ir-photoredox catalyzed Minisci C–H alkylation of heteroarenes with unactivated alkyl halides.

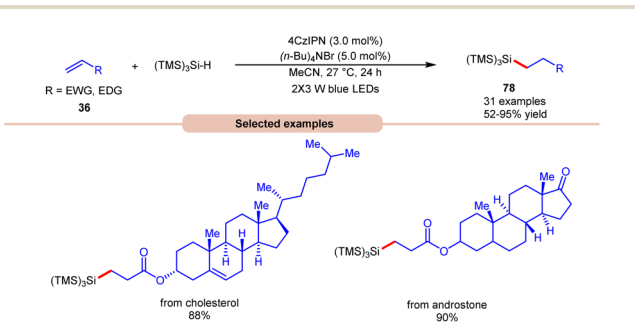

Scheme 30 Bromine radical-mediated hydrosilylation of alkenes using $(TMS)_3SiH$.

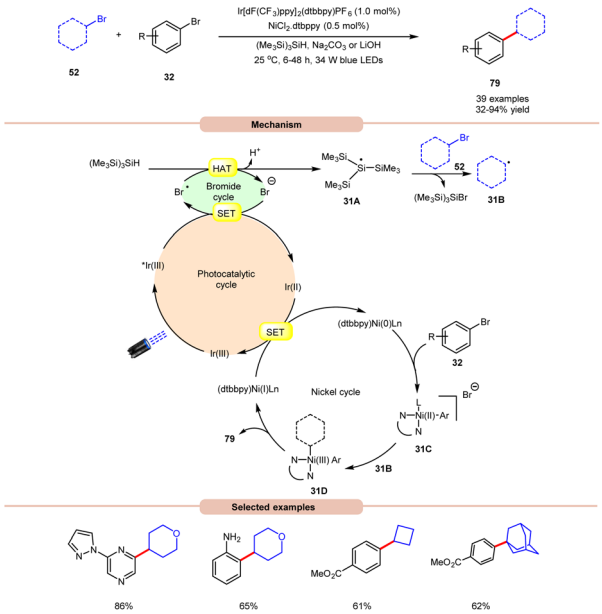

Scheme 31 Dual Ir/Ni-catalyzed approach towards the formation of a $C(sp^3)$–$C(sp^2)$ bond *via* cross-electrophile coupling between alkyl and aryl bromides.

bond *via* cross-electrophile coupling between alkyl **52** and aryl bromides **32** in good to excellent yields (Scheme 31).[39] The study of substrate scope showed that aryl bromide **32** featuring electron-rich and electron-deficient substituents was compatible with the given reaction conditions. Interestingly, an unprotected 2-bromo aniline substrate can be employed directly and give the corresponding product in 65% yield. Additionally, *N*-containing heterocycles such as pyrazine, pyrimidine, pyridazinequinolone, isoquinoline, and pyrazole-substituted pyrazine were well tolerated under the reaction conditions. Furthermore, cyclic and acyclic alkyl bromide **52** worked well. Mechanistically, the photoexcited *Ir(III)-complex oxidizes the bromide anion to generate a bromine radical *via* the SET process, which upon HAT from tris(trimethylsilyl) silane (TTMS) forms a stabilized silyl radical intermediate **31A**. Subsequently, silyl radical intermediate **31A** rapidly abstracts a halogen atom from the alkyl bromide **52** to form alkyl radical **31B** and the silyl bromide by-product. Moreover, a Ni(0)-complex undergoes oxidative addition with the aryl bromide **32** to form Ni(II) species **31C**, which then interacts with an alkyl radical **31B** to yield the Ni(III)-complex **31D**. The reductive elimination of **31D** delivers the desired $C(sp^3)$–$C(sp^2)$ cross-coupling product **79** and a Ni(I) intermediate, which continues the catalytic cycle.

In the extension of their previous work, MacMillan and co-workers in 2021 reported dual photoredox Ir/Ni-catalyzed cross-electrophile coupling between an alkyl halide **80** and a diverse range of aryl bromides **32** to produce artificial analogues of tryptophan, phenylalanine, and histidine derivatives (Scheme 32).[40] Various aryl bromides **32**, featuring electron-donating and electron-withdrawing groups, were successfully utilized, leading to the desired products **81** in moderate to excellent yields.

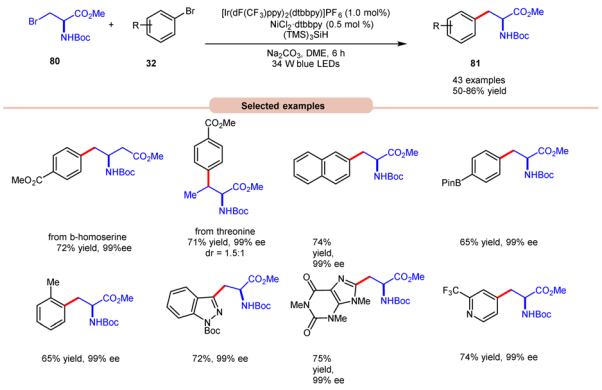

Scheme 32 Dual Ir/Ni-catalyzed cross-electrophile coupling between alkyl halides and a diverse range of aryl halides.

Additionally, substitution at the *ortho*-, *meta*-, and *para*-positions was well-accommodated, although *ortho*-substituted aryl halides **32** necessitated a higher loading of the nickel catalyst (5 mol%). Hong and co-workers achieved the synthesis of C_4-alkylated pyridines **83** through an EDA-complex between pyridinium salts **82** and bromide ions under visible-light irradiation (Scheme 33).[41]

A wide range of primary, secondary, and tertiary alkyl bromides **52** efficiently participated under the optimized conditions, yielding the desired products **83** in 40–91% yield. Initial experiments with a pyridinium salt and bromocyclohexane indicated that the *in situ* generated bromide anion effectively initiated a radical chain reaction under visible light irradiation, eliminating the need for an external bromide source. However,

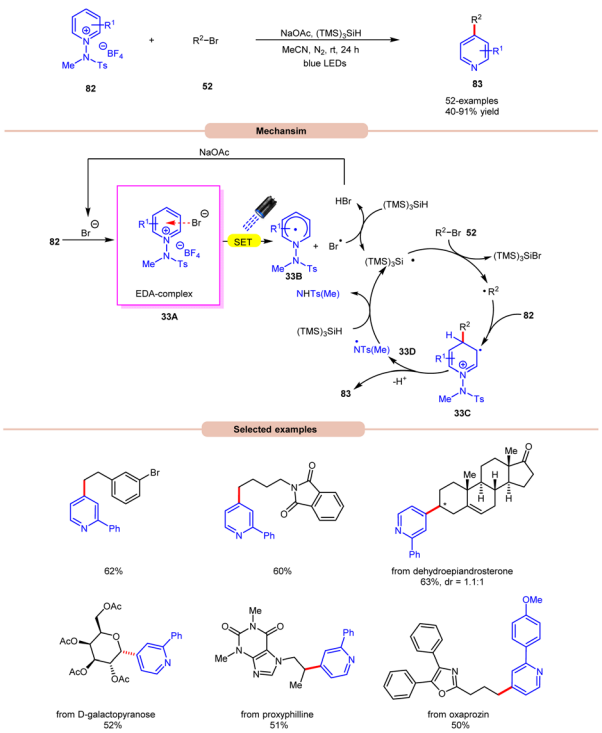

Scheme 33 Bromide anion catalyzed alkylation of a pyridinium salt.

employing tetrabutylammonium bromide (TBAB) as a bromide anion source resulted in reduced yields of the targeted product. UV-visible absorption studies confirmed the formation of an EDA complex between the bromine anion and pyridinium salt **82**. Stern–Volmer experiments revealed the formation of a bromine radical *via* reductive quenching of pyridinium salt **82** with the bromine anion. Moreover, the high quantum yield ($\Phi = 19.0$) supported the involvement of a radical chain pathway. Mechanistically, an EDA-complex **33A** is formed between the pyridinium salt (acceptor) **82** and bromide anion (donor). Visible light irradiation triggered a SET event, producing a bromine radical that initiated the chain reaction by abstracting an H-atom from $(TMS)_3SiH$. The resulting silyl radical captures the bromine atom from alkyl bromides **52** to generate the corresponding alkyl radical (R˙). This alkyl radical regioselectively adds to the C_4-position of the pyridinium salt **82**, followed by deprotonation and homolytic N–N bond cleavage to yield the desired C_4-alkylated pyridine product **83** and the regeneration of the silyl radical *via* N-centered radical intermediate **33D**, which propagates the chain.

6. Hydrogen atom transfer from allylic carbons

The allylic position is particularly reactive due to the stability of the resulting allylic radical, which is resonance-stabilized. Allylic hydrogen atom transfer can occur through radical reactions, where a bromine radical abstracts a hydrogen atom from the allylic carbon as shown in Scheme 34.

An acridinium and Ni-catalyzed cross-coupling reaction between allylic compounds **84** and arylbromides **32** was reported by Rueping and coworkers in 2018 (Scheme 35).[42] Under optimized reaction conditions, the oxidative addition of aryl bromide **32** to the Ni(0) complex gives a Ni(II) complex **35A**. Next, triplet–triplet energy transfer (EnT) occurred from the photoexcited catalyst *Mes-Acr-Me$^+$ and Ni(II) complex **35A** to give intermediate **35B**. After that, the excited form of Ni(II) complex **35B** undergoes homolytic bond cleavage of the Br–Ni bond and generates a bromine radical and a Ni(I) complex **35C**. The weak allylic C–H bond of alkene **84** undergoes H-atom transfer to the bromine atom and gives HBr and allylic radical **35D**. Lastly, reductive elimination occurs to give the final product **85**. This reaction is also compatible with vinyl bromides **34** to yield the desired products **86** in 51–64% yield.

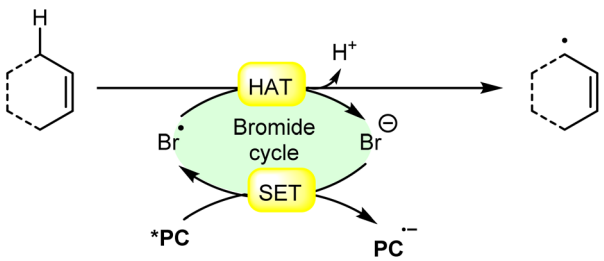

Scheme 34 General approach for allylic radical intermediate formation *via* bromine radical-mediated HAT.

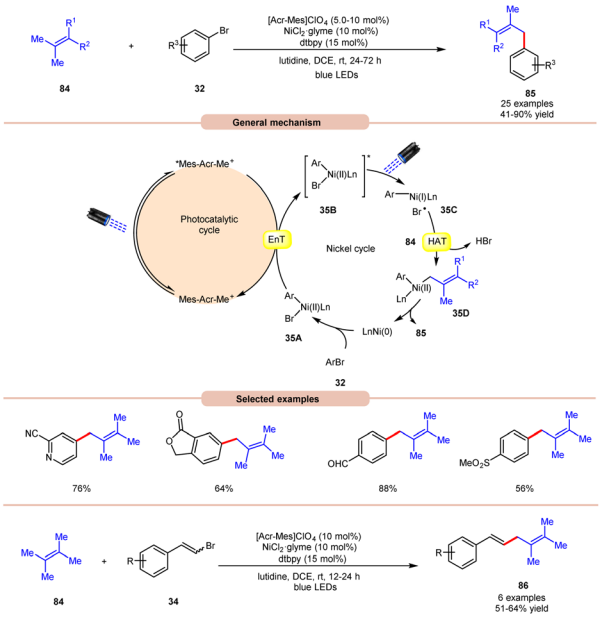

Scheme 35 Dual acridinium/Ni-catalyzed cross-coupling reaction between allylic compounds and aryl bromides.

Thereafter, a novel and efficient approach towards aerobic allylic C–H bond oxidation was achieved by Cai and co-workers in 2022 using nBu$_4$NBr as a bromide source, with rose bengal as a photocatalyst under visible light irradiation (Scheme 36).[43] This strategy was applicable to a wide range of tertiary cyclohexenol derivatives **87** as well as those containing 5, 7, and 8 membered cyclic ring and acyclic derivatives, affording the desired enone products **88** in 33–91% yield. The robustness of this photocatalytic aerobic reaction was also found compatible with a wide range of pharmaceutically active steroids and triterpene derivatives, resulting in the required products **88**. Detailed mechanistic studies were performed to gain insights into the reaction mechanism. Radical quenching with TEMPO and DABCO (singlet oxygen quencher) confirmed the involvement of singlet oxygen in the reaction protocol. Stern–Volmer experiments supported the higher quenching efficiency of molecular oxygen with rose bengal compared to other reactants. When performed in the absence of nBu$_4$NBr, the reaction resulted in the formation of a keto-acid product under similar conditions, indicating that singlet oxygen is formed in the reaction protocol and nBu$_4$NBr is important for product formation. Based on these studies, the authors proposed that the photoexcited catalyst *RB undergoes an EnT process with O_2 to form singlet oxygen ($^1O_2$), which itself participates in SET with a bromide anion to form a bromine radical and superoxide radical intermediate. Thereafter, substrate **87** undergoes HAT with the bromine radical to form C-centered radical intermediate **36A**. This intermediate reacts with the superoxide radical to form an anion intermediate **36B**. Finally, the protonation and elimination of H_2O give access to the final enone product **88**. This strategy offers a straightforward method for the allylic C–H oxidation of structurally challenging and complex molecules.

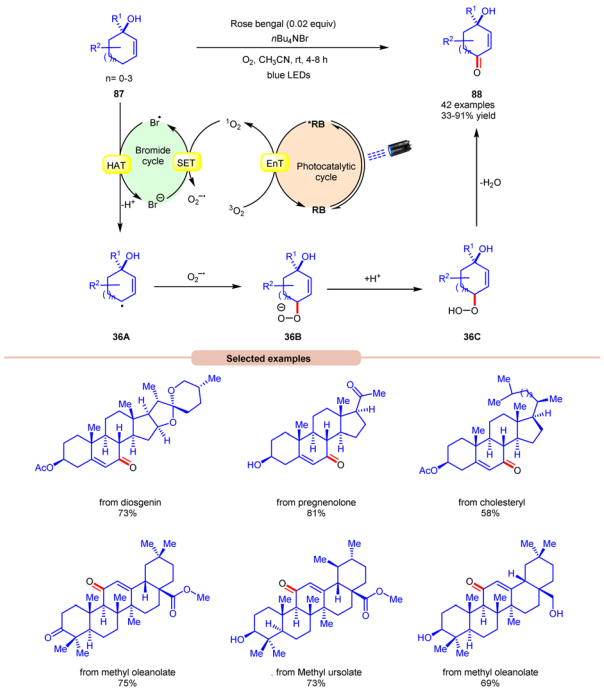

Scheme 36 Rose bengal mediated allylic oxidation for the synthesis of enones.

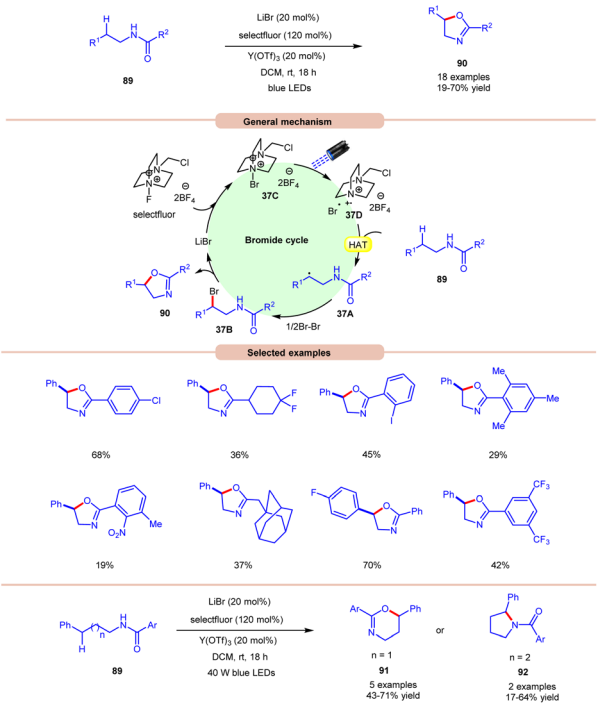

Scheme 37 Visible light-mediated bromine radical catalyzed synthesis of oxazolines, pyrrolidines, and dihydrooxazines.

7. Miscellaneous

Li and co-workers, in 2021, demonstrated bromide-catalyzed C–H functionalization of amide carbonyl carbon for the synthesis of oxazolines, pyrrolidines, and dihydrooxazines (Scheme 37).[44] For the synthesis of oxazolines, *N*-phenethylbenzamide derivative **89** was employed as a standard substrate with LiBr as a bromide catalyst with F-TEDA-BF_4 (selectfluor) as an oxidant and $Y(OTf)_3$ as an additive under visible light irradiation. An array of electron-donating and withdrawing functionalities on the *N*-phenethylbenzamide derivative **89** reacted smoothly to afford the desired product **90** in 19–70% yield. Notably, substrates bearing bulky arene groups such as 2,4,6-trimethyl or o-nitro or 3,5-CF_3 groups afforded the targeted products in diminished yields. Mechanistic studies reveal that visible light, selectfluor, and air were indispensable for the reaction. The generation of an *N*-centered radical intermediate was ruled out from selectfluor (N–F bond homolysis) since no product bearing fluorine groups were observed. From these observations, the authors proposed the formation of intermediate **37C** through the interaction between LiBr and selectfluor, which in the presence of light generates *N*-centered cation radial intermediate **37D** *via* fragmentation. Next, the *N*-phenethylbenzamide derivative **89** undergoes intermolecular HAT with the bromine radical to form C-centered radical intermediate **37A**. Next, bromination, accompanied by the subsequent cyclization and deprotonation, yields the desired oxazoline product **90** with the regeneration of the bromide catalyst. High loading of the catalyst and additive was the only limitation of this method. The authors further demonstrated the synthesis of dihydroxazines **91** and pyrroline **92** using this reaction protocol.

8. Conclusions

This article provides an overview of C–H activation reactions initiated by Br$^{\bullet}$ radicals generated through photocatalytic interactions with a catalyst under visible light irradiation. These Br$^{\bullet}$ radicals serve as appealing hydrogen atom transfer (HAT) reagents and electron acceptors due to their robust oxidative properties and the formation of strong covalent bonds with hydrogen atoms. Moreover, the efficient generation of Br$^{\bullet}$ radicals *via* light irradiation offers advantages in terms of reaction control. Compared to conventional synthetic methods, it can offer a more efficient and resource-conserving approach to constructing complex organic compounds. Despite the significant advancements made in this area, there are still many opportunities and challenges remaining, such as: (1) in this review article, the majority of the bromine radical mediated strategies are accelerated by expensive Ir-photoredox catalysis, sometimes in combination with nickel/ligand systems. This leaves room to explore other inexpensive metal and non-metal catalysts for their successful execution and ease the pathway to generate bromine radicals, which take part in the HAT reaction; (2) exploring electron-donor–acceptor (EDA) complex strategies and strategies involving visible light-mediated homolysis without the need for a photocatalyst for the generation of bromine radicals is highly desirable; (3) mainly, C–C, and C–O bond formation has been reported under these strategies; however, methods for the construction of C–N, C–S, C–P,

C–X (X = halides) are still unexplored by bromine radical ($Br^{\bullet}$) mediated HAT strategies. We hope that this review will stimulate interest in C–H activation reactions involving bromine radicals ($Br^{\bullet}$) *via* HAT and deepen the understanding of their reactivity, thereby aiding in their application across various academic and industrial levels.

Data availability

No primary research results, software or code have been included and no new data were generated or analysed as part of this review.

Conflicts of interest

The authors have no conflicts of interest.

Acknowledgements

Financial support from UCOST (UCS & T/R & D-35/20-21) Govt. of Uttarakhand, and SERB (CRG/2022/002691), India, is gratefully acknowledged. B. S. and R. P. thank CSIR and UGC for the SRF Fellowship, respectively.

References

1 (*a*) C. R. J. Stephenson, T. Yoon and D. W. C. Macmillan, in *Visible Light Photocatalysis in Organic Chemistry*, Wiley-VCH, German, 2018; (*b*) D. A. Nicewicz and D. W. C. MacMillan, *Science*, 2008, **322**, 77–80; (*c*) D. S. Hamilton and D. A. Nicewicz, *J. Am. Chem. Soc.*, 2012, **134**, 18577–18580; (*d*) L. Marzo, S. K. Pagire, O. Reiser and B. König, *Angew. Chem., Int. Ed.*, 2018, **57**, 10034–10072; *Angew. Chem.*, 2018, **130**, 10188–10228; (*e*) D. Ravelli, S. Protti and M. Fognoni, *Chem. Rev.*, 2016, **116**, 9850–9913; (*f*) X.-Y. Yu, J.-R. Chen and W.-J. Xiao, *Chem. Rev.*, 2021, **121**, 506–561; (*g*) R. I. Patel, S. Sharma and A. Sharma, *Org. Chem. Front.*, 2021, **8**, 3166–3200; (*h*) N. Kvasovs and V. Gevorgyan, *Chem. Soc. Rev.*, 2020, **50**, 2244–2259; (*i*) K. L. Skubi, T. R. Blum and T. P. Yoon, *Chem. Rev.*, 2016, **116**, 10035–10074; (*j*) A. Y. Chan, I. B. Perry, N. B. Bissonnette, B. F. Buksh, G. A. Edwards, L. I. Frye, O. L. Garry, M. N. Lavagnino, B. X. Li, Y. Liang, E. Mao, A. Millet, J. V. Oakley, N. L. Reed, H. A. Sakai, C. P. Seath and D. W. C. MacMillan, *Chem. Rev.*, 2022, **122**, 1485–1542; (*k*) T. Constantin, F. Julia and D. Leonori, *Chem. Rev.*, 2022, **122**, 2292–2352; (*l*) A. R. Allen, E. A. Noten and C. R. J. Stephenson, *Chem. Rev.*, 2022, **122**, 2695–2751; (*m*) K. P. S. Cheung, S. Sarkar and V. Gevorgyan, *Chem. Rev.*, 2022, **122**, 1543–1625; (*n*) S. P. Pitre and L. E. Overman, *Chem. Rev.*, 2022, **122**, 1717–1751; (*o*) L. Chang, Q. An, L. Duan, K. Feng and Z. Zuo, *Chem. Rev.*, 2022, **122**, 2429–2486; (*p*) K. Kwon, R. T. Simons, M. Nandakumar and J. L. Roizen, *Chem. Rev.*, 2022, **122**, 2353–2428; (*q*) L. Capaldo, D. Ravelli and M. Fagnoni, *Chem. Rev.*, 2022, **122**, 1875–1924; (*r*) A. Tlili and S. Lakhdar, *Angew. Chem., Int. Ed.*, 2021, **60**, 19526–19549; (*s*) A. Tlili and S. Lakhdar, *Angew. Chem., Int. Ed.*, 2021, **133**, 19678–19701; (*t*) R. I. Patel, J. Singh and A. Sharma, *ChemCatChem*, 2022, **14**, e202200260; (*u*) B. Saxena, R. I. Patel, J. Tripathi and A. Sharma, *Org. Biomol. Chem.*, 2023, **21**, 4723–4743.

2 (*a*) C. K. Prier, D. A. Rankic and D. W. C. MacMillan, *Chem. Rev.*, 2013, **113**, 5322–5363; (*b*) T. Koike and M. Akita, *Inorg. Chem. Front.*, 2014, **1**, 562–576; (*c*) K. Teegardin, J. I. Day, J. Chan and J. Weaver, *Org. Process Res. Dev.*, 2016, **20**, 1156–1163; (*d*) D. A. Nicewicz and T. M. Nguyen, *ACS Catal.*, 2014, **4**, 355–360; (*e*) D. P. Hari and B. König, *Chem. Commun.*, 2014, **50**, 6688–6699; (*f*) M. H. Shaw, J. Twilton and D. W. C. MacMillan, *J. Org. Chem.*, 2016, **81**, 6898–6926; (*g*) C.-S. Wang, P. H. Dixneuf and J.-F. Soulé, *Chem. Rev.*, 2018, **118**, 7532–7585; (*h*) S. Sharma and A. Sharma, *Org. Biomol. Chem.*, 2019, **17**, 4384–4405; (*i*) W. M. Cheng and R. Shang, *ACS Catal.*, 2020, **10**, 9170–9196; (*j*) R. I. Patel, A. Sharma, S. Sharma and A. Sharma, *Org. Chem. Front.*, 2021, **8**, 1694–1718.

3 (*a*) C. G. S. Lima, T. D. M. Lima, M. Duarte, I. D. Jurbery and M. W. Paixão, *ACS Catal.*, 2016, **6**, 1389; (*b*) Y. Q. Yuan, S. Majumder, M. H. Yang and S. R. Guo, *Tetrahedron Lett.*, 2020, **61**, 151506; (*c*) P. Garra, J. P. Fouassier, S. Lakhdar, Y. Yagci and J. Lalevée, *Prog. Polym. Sci.*, 2020, **107**, 101277; (*d*) G. E. M. Crisenza, D. Mazzarella and P. Melchiorre, *J. Am. Chem. Soc.*, 2020, **142**, 5461; (*e*) B. Saxena, R. I. Patel and A. Sharma, *Adv. Synth. Catal.*, 2023, **365**, 1538–1564.

4 (*a*) L. Troian-Gautier, M. D. Turlington, S. A. M. Wehlin, A. B. Maurer, M. D. Brady, W. B. Swords and G. J. Meyer, *Chem. Rev.*, 2019, **119**(7), 4628–4683; (*b*) S. Rohe, A. O. Morris, T. McCallum and L. Barriault, *Angew. Chem., Int. Ed.*, 2018, **57**, 15664–15669; (*c*) M. Zidan, A. O. Morris, T. McCallum and L. Barriault, *Eur. J. Org Chem.*, 2020, **2020**, 1453–1458; (*d*) H. P. Deng, Q. Zhou and J. Wu, *Angew. Chem.*, 2018, **130**, 12843–12847.

5 (*a*) B. J. Shields and A. G. Doyle, *J. Am. Chem. Soc.*, 2016, **138**, 12719–12722; (*b*) M. K. Nielsen, B. J. Shields, J. Liu, M. J. Williams, M. J. Zacuto and A. G. Doyle, *Angew. Chem., Int. Ed.*, 2017, **56**, 7191–7194; (*c*) S. K. Kariofillis, B. J. Shields, M. A. Tekle-Smith, M. J. Zacuto and A. G. Doyle, *J. Am. Chem. Soc.*, 2020, **142**, 7683–7689; (*d*) L. K. G. Ackerman, J. I. M. Alvarado and A. G. Doyle, *J. Am. Chem. Soc.*, 2018, **140**, 14059–14063; (*e*) Y. Jin, Q. Zhang, L. Wang, X. Wang, C. Meng and C. Duan, *Green Chem.*, 2021, **23**, 6984–6989.

6 (*a*) J. M. Mayer, *Acc. Chem. Res.*, 2011, **44**(1), 36–46; (*b*) L.-M. Zhao, Q.-Y. Meng, X.-B. Fan, C. Ye, X.-B. Li, B. Chen, V. Ramamurthy, C.-H. Tung and L.-Z. Wu, *Angew. Chem., Int. Ed.*, 2017, **56**, 3020–3024; (*c*) T. Ide, J. P. Barham, M. Fujita, Y. Kawato, H. Egami and Y. Hamashima, *Chem. Sci.*, 2018, **9**, 8453–8460; (*d*) E. L. Saux, M. Zanini and P. Melchiorre, *J. Am. Chem. Soc.*, 2022, **144**, 1113–1118; (*e*) T. Uchikura, K. Tsubono, Y. Hara and T. Akiyama, *J. Org. Chem.*, 2022, **87**, 15499–15510; (*f*) G. Kumar, S. Pradhan and I. Chatterjee, *Chem.–Asian J.*, 2020, **15**, 651–672.

7 (*a*) H. P. Deng, X. Z. Fan, Z. H. Chen, Q. H. Xu and J. Wu, *J. Am. Chem. Soc.*, 2017, **139**, 13579–13584; (*b*) C. Y. Huang, J. Li and C. J. Li, *Nat. Commun.*, 2021, **12**, 4010.

8 (*a*) S. J. Blanksby and G. B. Ellison, *Acc. Chem. Res.*, 2003, **36**, 255–263; (*b*) Y. Shen, Y. Gu and R. Martin, *J. Am. Chem. Soc.*, 2018, **140**, 12200–12209; (*c*) J. A. Kerr, *Chem. Rev.*, 1966, **66**(5), 465–500; (*d*) X.-S. Xue, P. Ji, B. Zhou and J.-P. Cheng, *Chem. Rev.*, 2017, **117**(13), 8622–8648.

9 (*a*) L. Capaldo, L. L. Quadri and D. Ravelli, *Green Chem.*, 2020, **22**, 3376–3396; (*b*) L. Capaldo, D. Ravelli and M. Fagnoni, *Chem. Rev.*, 2022, **122**(2), 1875–1924; (*c*) H. Cao, X. Tang, H. Tang, Y. Yuan and J. Wu, *Chem Catal.*, 2021, **1**, 523–598; (*d*) H. Chena and S. Yu, *Org. Biomol. Chem.*, 2020, **18**, 4519–4532.

10 S. Bonciolini, T. Noël and L. Capaldo, *Eur. J. Org Chem.*, 2022, e202200417.

11 Y. Itabashi, H. Asahara and K. Ohkubo, *Chem. Commun.*, 2023, **59**, 7506–7517.

12 Z. Wang, Q. Liu, X. Ji, G.-J. Deng and H. Huang, *ACS Catal.*, 2020, **10**, 154–159.

13 X. Ji, Q. Liu, Z. Wang, P. Wang, G.-J. Deng and H. Huang, *Green Chem.*, 2020, **22**, 8233–8237.

14 (*a*) K. Ding, Y. Lu, Z. Nikolovska-Coleska, G. Wang, S. Qiu, S. Shangary, W. Gao, D. Qin, J. Stuckey, K. Krajewski, P. P. Roller and S. Wang, *J. Med. Chem.*, 2006, **49**, 3432–3435; (*b*) S. Peddibhotla, *Curr. Bioact. Compd.*, 2009, **5**, 20; (*c*) A. Millemaggi and R. J. K. Taylor, *Eur. J. Med. Chem.*, 2010, **2010**, 4527–4547; (*d*) M. Kaur, M. Singh, N. Chadha and O. Silakari, *Eur. J. Med. Chem.*, 2016, **123**, 858–894; (*e*) B. Yu, D.-Q. Yu and H.-M. Liu, *Eur. J. Med. Chem.*, 2015, **97**, 763–798; (*f*) N. Ye, H. Chen, E. A. Wold, P. Y. Shi and J. Zhou, *ACS Infect. Dis.*, 2016, **2**, 382–392.

15 Z. Sun, H. Huang, Q. Wang, C. Huang, G. Mao and G.-J. Deng, *Org. Chem. Front.*, 2022, **9**, 3506–3514.

16 (*a*) H. Wang, H. Liu, M. Wang, M. Huang, X. C. Shi, T. Wang, X. Cong, J. Yan and J. Wu, *iScience*, 2021, **24**(6), 102693; (*b*) T. Ye, Y. Li, Y. Ma, S. Tan and F. Li, *J. Org. Chem.*, 2024, **89**, 534–540.

17 T. Kawasaki, N. Ishida and M. Murakami, *J. Am. Chem. Soc.*, 2020, **142**, 3366–3370.

18 (*a*) T. Kawasaki, N. Ishida and M. Murakami, *Angew. Chem., Int. Ed.*, 2020, **59**, 18267–18271; (*b*) T. Kawasaki, T. Tosaki, N. Ishida and M. Murakami, *Org. Lett.*, 2021, **23**, 7683–7687.

19 Q.-L. Wang, H. Huang, Z. Sun, Y. Chen and G.-J. Deng, *Green Chem.*, 2021, **23**, 7790–7795.

20 H. Yu, T. Zhan, Y. Zhou, L. Chen, X. Liu and X. Feng, *ACS Catal.*, 2022, **12**, 5136–5144.

21 Q.-L. Wang, H. Huang, M. Zhu, T. Xu, G. Mao and G.-J. Deng, *Org. Lett.*, 2023, **25**, 3800–3805.

22 Q.-L. Wang, H. Huang, G. Mao and G.-J. Deng, *Green Chem.*, 2022, **24**, 8324–8329.

23 Q.-L. Wang, Z. Sun, H. Huang, G. Mao and G.-J. Deng, *Green Chem.*, 2022, **24**, 3293–3299.

24 (*a*) M. B. Smith and J. March, *March's Advanced Organic Chemistry: Reactions, Mechanisms, and Structure*, John Wiley & Sons, Hoboken, NJ, 2013; (*b*) R. Álvarez, B. Vaz, H. Gronemeyer and A. R. de Lera, *Chem. Rev.*, 2014, **114**, 1–125; (*c*) M. Hassam, A. Taher, G. E. Arnott, I. R. Green and W. A. L. Van Otterlo, *Chem. Rev.*, 2015, **115**, 5462–5569; (*d*) B. E. Maryanoff and A. B. Reitz, *Chem. Soc. Rev.*, 1989, **89**, 863–927; (*e*) P. A. Byrne and D. G. Gilheany, *Chem. Soc. Rev.*, 2013, **42**, 6670–6696; (*f*) H.-T. Chang, T. T. Jayanth, C.-C. Wang and C.-H. Cheng, *J. Am. Chem. Soc.*, 2007, **129**, 12032–12041; (*g*) C. W. Cheung, F. E. Zhurkin and X. Hu, *J. Am. Chem. Soc.*, 2015, **137**, 4932–4935; (*h*) B. Saxena, R. I. Patel, S. Sharma and A. Sharma, *Green Chem.*, 2024, **26**, 2721–2729; (*i*) Y. Ikeda, T. Nakamura, H. Yorimitsu and K. Oshima, *J. Am. Chem. Soc.*, 2002, **124**, 6514–6515; (*j*) W. Affo, H. Ohmiya, T. Fujioka, Y. Ikeda, T. Nakamura, H. Yorimitsu, K. Oshima, Y. Imamura, T. Mizuta and K. Miyoshi, *J. Am. Chem. Soc.*, 2006, **128**, 8068–8077; (*k*) K. Zhu, J. Dunne, M. P. Shaver and S. P. Thomas, *ACS Catal.*, 2017, **7**, 2353–2356; (*l*) S. J. Meek, R. V. O'Brien, J. Liaveria and R. R. Schrock, *Nature*, 2011, **471**, 461–466; (*m*) T. Di Franco, A. Epenoy and X. Hu, *Org. Lett.*, 2015, **17**, 4910–4913; (*n*) Q. Liu, X. Dong, J. Li, J. Xiao, Y. Dong and H. Liu, *ACS Catal.*, 2015, **5**, 6111–6137.

25 X. Cheng, T. Li, Y. Liu and Z. Lu, *ACS Catal.*, 2021, **11**, 11059–11065.

26 P. Jia, Q. Li, W. C. Poh, H. Jiang, H. Liu, H. Deng and J. Wu, *Chem*, 2020, **6**, 1766–1776.

27 Z. Wang, X. Ji, T. Han, G.-J. Deng and H. Huang, *Adv. Synth. Catal.*, 2019, **361**, 5643–5647.

28 (*a*) C.-L. Cao, G.-X. Zhang, F. Xue and H.-P. Deng, *Org. Chem. Front.*, 2022, **9**, 959–965; (*b*) Y. Lin, X. Shu and H. Huo, *Synthesis*, 2024, **56**, 1702–1710.

29 (*a*) A. Butler and J. V. Walker, *Chem. Rev.*, 1993, **93**, 1937–1944; (*b*) D. Kahne, C. Leimkuhler, W. Lu and C. Walsh, *Chem. Rev.*, 2005, **105**, 425–448; (*c*) F. H. Vaillancourt, E. Yeh, D. A. Vosburg, S. Garneau-Tsodikova and C. T. Walsh, *Chem. Rev.*, 2006, **106**, 3364–3378; (*d*) C. Paul and G. Pohnert, *Nat. Prod. Rep.*, 2011, **28**, 186–195; (*e*) J. Latham, E. Brandenburger, S. A. Shepherd, B. R. K. Menon and J. Micklefield, *J. Chem. Rev.*, 2018, **118**, 232–269.

30 Y. Chen, Z. Qu, S. Chen, X. Ji, G.-J. Deng and H. Huang, *Adv. Synth. Catal.*, 2022, **364**, 1573–1579.

31 M. S. Santos, M. Cybularczyk-Cecotka, B. König and M. Giedyk, *Chem.–Eur. J.*, 2020, **26**, 15323–15329.

32 M. S. Santos, A. G. Corrêa, M. W. Paixão and B. König, *Adv. Synth. Catal.*, 2020, **362**, 2367–2372.

33 (*a*) C.-H. Qu, R. Huang, Y. Liu, T. Liu and G.-T. Song, *Org. Chem. Front.*, 2022, **9**, 4135–4145; (*b*) B. Sun, P.-X. Li, Y. Jiang, L.-L. Yang, P.-Y. Huang, R.-P. Shen, M.-J. Chen, J.-Y. Wang and C. Jin, *Org. Lett.*, 2023, **25**, 6773–6778.

34 C. Wang, H. Shi, G.-J. Deng and H. Huang, *Org. Biomol. Chem.*, 2021, **19**, 9177–9181.

35 S. K. Kariofillis, S. Jiang, A. M. Żurański, S. S. Gandhi, J. I. M. Alvarado and A. G. Doyle, *J. Am. Chem. Soc.*, 2022, **144**, 1045–1055.

36 A. ElMarrouni, C. B. Ritts and J. Balsells, *Chem. Sci.*, 2018, **9**, 6639–6646.

37 J. Dong, X. Lyu, Z. Wang, X. Wang, H. Song, Y. Liua and Q. Wang, *Chem. Sci.*, 2019, **10**, 976–982.

38 Y. Zhao, K. Zhang, Y. Bai, Y. Zhang and S. Shi, *Chin. J. Inorg. Chem.*, 2023, **43**, 2837–2847.

39 P. Zhang, C. Chip Le and D. W. C. MacMillan, *J. Am. Chem. Soc.*, 2016, **138**(26), 8084–8087.
40 T. M. Faraggi, C. Rouget-Virbel, J. A. Rincón, M. Barberis, C. Mateos, S. García-Cerrada, J. Agejas, O. de Frutos and D. W. C. MacMillan, *Org. Process Res. Dev.*, 2021, **25**, 1966–1973.
41 S. Jung, S. Shin, S. Park and S. Hong, *J. Am. Chem. Soc.*, 2020, **142**, 11370–11375.
42 L. Huang and M. Rueping, *Angew. Chem., Int. Ed.*, 2018, **57**, 10333–10337.
43 C. Liu, H. Liu, X. Zheng, S. Chen, Q. Lai, C. Zheng, M. Huang, K. Cai, Z. Cai and S. Cai, *ACS Catal.*, 2022, **12**, 1375–1381.
44 N. Kaur, E. C. Ziegelmeyer, O. N. Farinde, J. T. Truong, M. M. Huynh and W. Li, *Chem. Commun.*, 2021, **57**, 10387–10390.